An underactuated gripper mechanism for picking objects from a tabletop

Mechanical Engineering, Delft Biorobotics Laboratory, TU Delft
Jelmer Korstanje, Advisor: Dr. ir. Martijn Wisse

***Abstract*— Underactuated grippers that are designed for the pick and place industry tend to pull objects into the gripper when a firm grip is required. This movement within the gripper is sometimes undesired and can damage the object. Therefore, the goal of this study is to design an underactuated gripper mechanism that is able to establish a final and stable grasp without moving the object. The objects are laying on a flat surface and should be grasped from above without damaging the object. By examining the grasping process, we determine the elements needed to create the new gripper mechanism. A mathematical model and simulation tool are developed to study the grasp performance of the gripper. The gripper performance is measured as the feasible grasp range with respect to the complete grasp range. The complete grasp range is determined by an object size range and a horizontal displacement of the object. We optimise the design parameters of the gripper for maximum gripper performance whilst a minimum coefficient of friction is present. With this gripper mechanism, we created a gripper that can cope with large variance in object size and that outperforms a pinch gripper when low contact friction force is required.**

***Index Terms*— Pick and place industry, grasping, underactuation, force equilibrium, friction forces**

1 INTRODUCTION

THE pick and place industry is in need for a mechanical end-effector that can handle irregular, delicate and fragile products. An end-effector is the part of an automation system that makes physical contact with the object to be handled. Nowadays, mechanical end-effectors like linear grippers and vacuum grippers are often being used to grasp and handle objects. Although these end-effectors have proven to be very useful, they are only effective for a small range of products. Since automation is more and more being applied to industry, also the variety of products to be handled is increasing. There is an increasing demand for grippers that can handle a complete object range, where the objects vary in shape and size. By means of many sensors, actuators and a control system, an end-effector can be created that is able to handle most products. However in industry a complex and expensive end-effector is not desirable. Therefore, a new type of mechanical gripper was introduced, the underactuated gripper. Examples of underactuated grippers especially designed for industry can be found in Fig. 1. A gripper is underactuated when it has more degrees of freedom (DOF) than numbers of actuators. It allows the gripper to be designed in such a way, that the gripper intrinsically adapts its configuration and is able to grasp different shaped objects without the need of a sensory system.

A disadvantage of these underactuated grippers is that when they are used to establish a firm grasp, small objects will be pulled into the gripper, as is demonstrated in Fig. 2. The movement of the object within the gripper sometimes damages a product. When the object finally is released again, the object can not be placed onto a surface, but has to be released above the surface and falls out of the gripper. This can result in a positioning error of the object. More recently, another underactuated gripper was designed for industry by Kragten et all. [3]. This gripper design automatically grasps small objects with only the tips of the gripper, a so called precision grasp is established. These grippers are also referred to as pinch grippers. This type of grasp heavily relies on friction forces, which causes a problem when: (1) delicate products are being handled that get easily damaged by shear forces, (2) pollution, like water or dirt, gets between the gripper and object and reduces the friction forces.

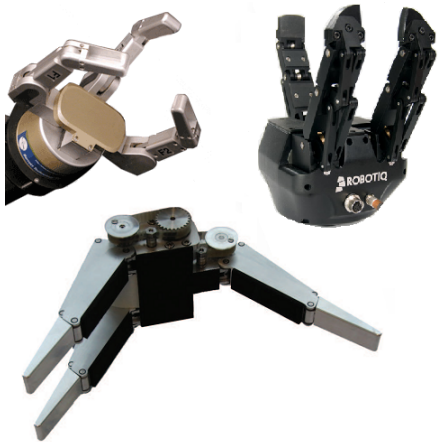

Figure 1: Underactuated robotic hands that were designed for industrial applications. Left top: BarretHand [12], right top: ROBOTIQ Adaptive Gripper [11] , bottom: Delft Hand 2 [9]

The objective of this research is to develop an underactuated gripper mechanism with which a final and stable grasp can be established without moving the object. This gripper mechanism should make it possible to grasp and release delicate and fragile products from and onto a flat surface, without damaging the product. The products vary in shape and size and should be approached from above since neighbouring products might prohibit access from the sides.

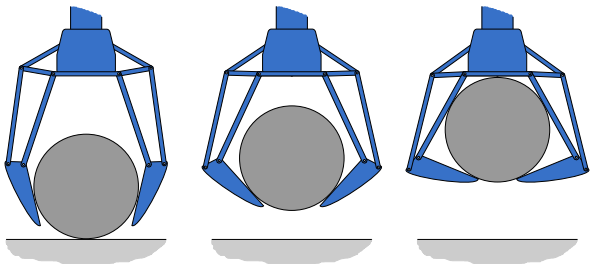

Figure 2: Sequence of images where an object is being pulled into a gripper during the grasping process.

The structure of this paper is as follows. Section 2 presents a complete model of the gripper design. The design choices on the configuration of the CE and actuation mechanism that are made to obtain the final model, are elaborated in this section as well. Section 3 gives a force analysis of the created model and some dimensional design choices are discussed. These elements are combined and finally the performance of the gripper is evaluated. In Sect. 4 we investigate the influence of static friction on the grasp performance. In Sect. 5 we use the performance evaluation from Sect. 4 to create an optimization method for the design parameters of the gripper. This allows the design of a gripper that shows optimal grasp performance with respect to the objective for a given product range. Following are the discussion and conclusion in respectively Sect 6 and 7.

2 Design

The goal of this section is to present a new underactuated gripper concept. To be able to design a new gripper concept, we first analyse the grasping process of underactuated grippers and the elements involved. To get a better understanding of the complex behavior of an underactuated gripper, we divide the gripper mechanism into two parts, the configuration of the connecting elements (CE) and the configuration of the actuation mechanism. The CE are the parts of the gripper that are designed to get in contact with the object. The actuation mechanism distributes the actuation force from the actuator over the CE.

The outline of the remainder of this section is as follows. First some designs simplifications are introduced in Sect. 2.1. Subsequently, the most important design requirements and choices for the configuration of the CE are discussed in Sect. 2.2. This is then repeated for the actuation mechanism in Sect. 2.3. Finally, in Sect. 2.4 the configuration of the CE and actuation mechanism are combined into a complete model.

2.1 Design simplifications

Due to the complex nature of underactuated grippers, we introduce some design simplifications. In this work, we use similar design simplifications as were used in earlier studies on underactuated grippers [3], [9].

Model simplification:
As in the design of the Delft Hand 2 [9], the final design of the gripper consists out of three identical gripping elements. Two of these elements have the same working direction and the third element is opposing the other two (see Fig. 1). This configuration can be seen as two fingers of a hand with an opposing thumb. The force distribution is such that the force applied by both fingers together equals the force applied by the opposing thumb. For modeling of the Delft Hand 2, a planar design is used with only two identical opposing fingers. In this research, we apply the same method. The model is only considered in a plane and two opposing, equally driven gripping elements are used.

Element properties:
All elements used in the design, are rigid and have zero thickness.

Friction force:
The objective is to create a gripper design where friction forces are kept to a minimum. This can be achieved by using a material for the CE that has a very low coefficient of friction. In the model of the gripper design, we neglect the friction force to ensure that the proper working of the gripper does not depend on friction force.

2.2 Connecting elements

With most underactuated hands or grippers, the term phalanges is used for the elements that are designed to get in contact with the object. This refers to the finger bones of the human hand, which often is a source of inspiration for the design of these grippers. In this work, we use the term *connecting elements* (CE), because thinking about human hands might limit the design solutions.

The shape of the gripper is mainly determined by the configuration of the CE. Therefore, we will now discuss the amount of CE needed to completely constrain an object and what type of CE we use.

Amount of CE:
To create a robust grasp, the CE should enclose the object [1]. The contact points between the CE and object are modeled as frictionless contact points that can exert only compressive forces. According to Reuleaux [10], at least 4 frictionless contact points that can exert arbitrary compressive forces are needed to completely restrain an object in a plane (2-dimensional). For an extensive proof, see [7]. It needs to be noted, that rotational symmetric objects can not completely be restrained by frictionless contact points since no contact is able to prohibit a rotation around the central axis of the object.

Type of CE:
There are two types of CE, fixed and movable CE. The fixed CE are rigidly connected to the base of the gripper and can not move with respect to the base. These elements can also be seen as part of the base. Movable CE are connected directly or indirectly to the base and can translate and/or rotate with respect to the base. When comparing translating and rotating CE, the following information needs to be taken into account:

- Rotating elements exert a contact force that depends on the contact location of object and CE, whereas translating elements exert a constant contact force over the whole contact area.
- To create a translating CE, some sort of guiding system or complex bar mechanism is needed.

The gripper is designed for being used in industry. Therefore, we try to realise the most simple and cheap grasping

solution. The most important design objective is that the final grasp should be established without moving the object. This means that the object should not move upwards or sideways when the gripper closes. For the design, this means that all the CE should be able to move with respect to the object. A fixed CE can only move with respect to the object by moving the whole gripper. This would mean a sensory system is needed for positioning the whole gripper. The actual goal is to create a gripper that works without a complex sensory system. From this, we conclude that fixed CE are not suitable for this gripper.

Since shape and size of the object may vary, it is best to use 4 individual movable CE to create 4 contact points with the object. A single CE that creates multiple contact points will sooner result in a restriction on object size than when each contact point is established by a single movable CE. Figure 3 shows a list of CE configurations, each CE configuration consists out of 4 CE and can completely restrain an object. A more elaborated overview can be found in Appendix A.

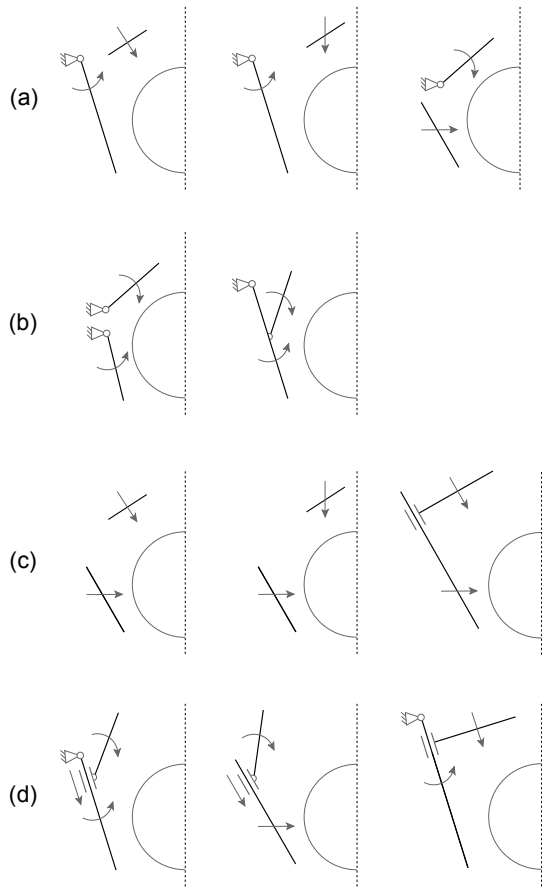

Figure 3: Four groups with gripper configurations that can completely restrain an object, where a) is a group with three different CE configurations that all consist out of two rotating CE and two translating CE, b) is a group with two different CE configurations that both consist out of four rotating CE, c) is a group with three different CE configurations that both consist out of four translating CE, d) is a group with three different CE configurations that all consist out of four CE where two CE are able to rotate as well as translate.

2.3 Actuation mechanism

The actuation mechanism combined with the actuator are the driving part of the gripper. The idea is to drive all the CE with just one single actuator. We will now discuss what actuation mechanism we use to distribute the actuation force over the CE.

According to Krut [6], three different types of underactuated mechanisms can be distinguished:

- Differential mechanisms: using any type of differential mechanism, one input is converted into multiple outputs.
- Compliant mechanisms: an additional degree of freedom is created by using non-rigid bodies [8].
- Triggered mechanisms: the degree of underactuation changes during the grasping process, e.g. a locking mechanism reduces a degree of freedom of the system after a given torque threshold has been reached.

In this study, we only focus on grippers that are driven by electrical motors and achieve underactuation by means of differential mechanisms. We can separate the distribution of the actuation force into two parts: *(1)* The distribution of the actuation force over the left and right part of the gripper. *(2)* The distribution of the actuation force of one half of the gripper over the belonging CE. For the distribution of the actuation force over the left and right half of the gripper, we use the same differential mechanism as was used in the Delft Hand 3 [3]. This is a patented technology and makes sure both halves of a gripper receive the same actuation force. The focus of this chapter will only be on distributing the actuation force of one side of the gripper over the corresponding CE. For this, we can use the following differential mechanisms (see Fig. 4):

- Cable-pulley mechanism: a cable and two pulleys transfer the actuation forces over the CE. There is a constant transmission ratio that is determined by the radii of the pulleys.
- Cam-tendon mechanism: two cams and a cable transfer the actuation forces over the CE. The force distribution over the CE is not constant and depends on the shape of both cams.
- Gear differential: the actuation force is transfered over the CE by several connected gears. The transmission ratio is determined by the gear ratio of the gear train.
- Bar-linkage mechanism: a framework of linkages transfers the actuation force over the CE. The transmission ratio is influenced by the length and orientation of the individual linkages.

The mechanisms shown in Fig. 4 all have two DOF and only one actuation input is needed to drive both DOF. Due to negative experience with cable/tendon systems in the past, we decide against the use of a cable/tendon system. Since the gripper is force controlled instead of position controlled, it is favorable for the proper working of the gripper to have as little friction as possible in the mechanism. Gear differential mechanisms are subjected to high friction forces and therefore we choose to make use of a bar-linkage differential mechanism.

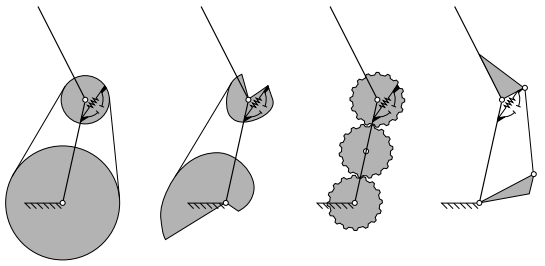

Figure 4: Four different differential mechanisms to actuate two linkages connected with a single joint. From the left to the right: cable-pulley, cam-tendon, gear differential and bar-linkage mechanism [6] .

The actuation force distributed to one CE relative to the actuation force distributed to the other CE, is called the transmission ratio [2]. The transmission ratio is mainly determined by the design of the actuation mechanism, which can be made such that the transmission ratio is a constant or depends on some variables in the system, e.g. the orientation of the CE. The transmission ratio has a large influence on the grasp behavior of the gripper. According to [5], the grasp configuration that results in force equilibrium of gripper and object, is mainly determined by the transmission ratio.

2.4 Gripper concept

One of the CE configurations from Fig. 3 is now combined with a bar-linkage differential mechanism to form the new gripper design. It is opted for to design a gripper with as few linkages and joints as possible. This results in a simple gripper design with low production costs. Since the gripper is force controlled instead of position controlled, friction forces in the system should be kept to a minimum. Therefore, we do not choose CE configurations with a sliding mechanism. This leaves us with only two options from the possible CE configurations. The final design of the gripper mechanism can be seen in Fig. 5. It consist out of merely rotating linkages (with respect to each other), it has 4 CE and therefore should be able to completely restrain an object. To distinguish between the several CE, from now on we call the CE that make contact with the lower side of the object *lower connecting elements* (LCE) and the CE that make contact at the upper side of the object *upper connecting elements* (UCE). The CE are connected such that the UCE is part of the actuation mechanism, therefore very few linkage are needed for the complete system. A spring is positioned between the LCE and UCE, see Fig. 5, to ensure that the initial contact of the gripper and object will be with the LCE. When the LCE is in contact with the object, the gripping strength increases and the resistance of the spring is overcome. The UCE starts to rotate with respect to the LCE and also makes contact with the object. The gripper is dimensioned by the design parameter set S,

$$\mathbf{S} = \{L_0, L_1, L_2, L_3, L_4, L_5, L_6, L_7, L_8\} \qquad (1)$$

The design parameters are shown in Fig. 6. In this figure, also the actuation torque from the actuator that is distributed over both halves of the gripper is represented, it is denoted by T_a which is a constant torque active on the linkage with parameter L_6.

2.5 Conclusion

The model of the final gripper design consists out of 4 rotating CE. Therefore, it should be able to completely constrain an object without moving it. A bar-linkage mechanism distributes the actuation force over the CE.

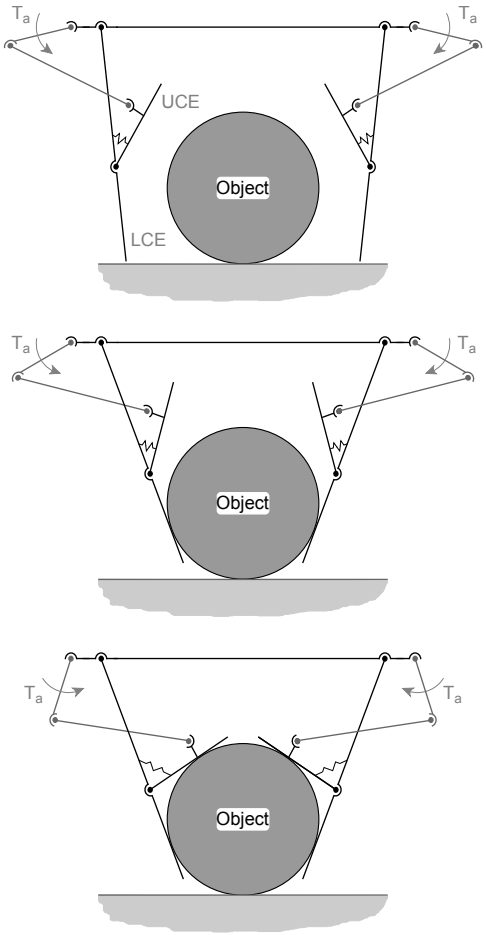

Figure 5: Representation of the grasping sequence of the new gripper design. The gripper grasps an object from above that is positioned on a table top. First the LCE and UCE rotate as one part, ensuring first contact is made with the LCE. Subsequently, the spring force of the spring connected between the LCE and UCE is overcome by the actuation force active on the UCE. The UCE starts to rotate with respect to the LCE and makes contact with the object as well. Final design of the gripper model.

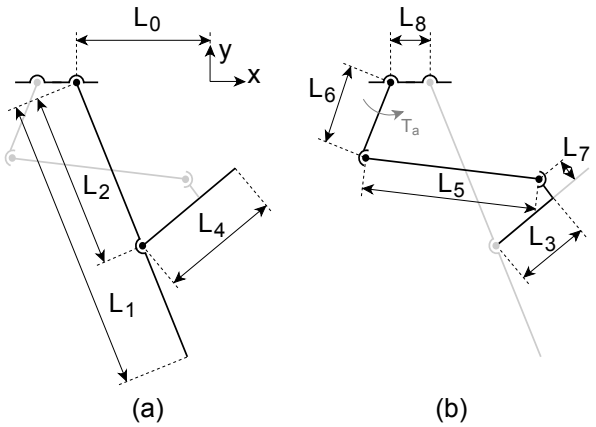

Figure 6: Schematic with design parameters of (a) the configuration of the CE. (b) the configuration of the actuation mechanism.

3 MODEL

The goal of this section is to investigate whether the presented gripper mechanism of the previous section can establish a final stable grasp without moving the object. In other words, we test the performance of the gripper mechanism towards the research objective.

In Sect. 3.1 a mathematical model is composed that describes the configuration of the gripper when the gripper is in contact with an object. Section 3.2 describes the important aspects for a proper dimensioning of the design parameters. In Sect. 3.3 we investigate whether force equilibrium of gripper and object is possible with the new gripper mechanism. In Sect. 3.4 the stability of an established grasp is determined.

3.1 Mathematical model

For the creation of the mathematical model of the gripper mechanism, the objects are modeled as massless cylindrical objects that are positioned in the centre of the gripper.

The creation of the mathematical model is performed in two steps. *(1)* We determine the configuration of the CE when the gripper is in contact with the object. *(2)* We determine the configuration of the actuation mechanism.

Configuration of the CE:

The configuration of the CE, when the gripper is in contact with the object, is described by the two independent variables θ_1 and θ_2 (see Fig. 7). We obtain an expression for θ_1 and θ_2 by rewriting the following loop closure vector equations that describe the configuration of the gripper in contact with the object. For the contact between the LCE and object:

$$\begin{pmatrix} -L_0 \\ 0 \end{pmatrix} + \mathbf{R}_{\theta_1} \begin{pmatrix} 0 \\ -p_1 \end{pmatrix} = \begin{pmatrix} X_{obj} \\ Y_{obj} \end{pmatrix} + \mathbf{R}_{\theta_1} \begin{pmatrix} -r_{obj} \\ 0 \end{pmatrix} \tag{2}$$

and for the contact between the UCE and the object:

$$\begin{pmatrix} -L_0 \\ 0 \end{pmatrix} + \mathbf{R}_{\theta_1} \begin{pmatrix} 0 \\ -L_2 \end{pmatrix} + \mathbf{R}_{\theta_1}\mathbf{R}_{\theta_2} \begin{pmatrix} 0 \\ -p_2 \end{pmatrix} = \begin{pmatrix} X_{obj} \\ Y_{obj} \end{pmatrix} + \mathbf{R}_{\theta_1}\mathbf{R}_{\theta_2} \begin{pmatrix} r_{obj} \\ 0 \end{pmatrix} \tag{3}$$

Here, p_1 is the point on the LCE where the LCE and the object make contact, p_2 is the point on the UCE where the UCE and the object make contact, X_{obj} and Y_{obj} are the coordinates of the object with respect to the gripper base, r_{obj} is the radius of the object, and $\mathbf{R}_{\theta_i}$ is the rotation matrix. The loop closure vector equations give 4 equations and 4 unknown, i.e. θ_1, θ_2, p_1 and p_2. Rewriting the loop closure vector equations (see Appendix B) gives the following expression for θ_1 and θ_2 ,

$$\theta_1 = \arccos\left(\frac{r_{obj}}{\sqrt{(X_{obj}+L_0)^2+Y_{obj}^2}}\right) + \arctan\left(\frac{Y_{obj}}{X_{obj}+L_0}\right) \tag{4}$$

$$\theta_2 = \arccos\left(\frac{-r_{obj}}{\sqrt{(X_{obj}+L_0-L_2\sin\theta_1)^2+(Y_{obj}+L_2\cos\theta_1)^2}}\right) + \arctan\left(\frac{Y_{obj}+L_2\cos\theta_1}{X_{obj}+L_0-L_2\sin\theta_1}\right) - \theta_1 \tag{5}$$

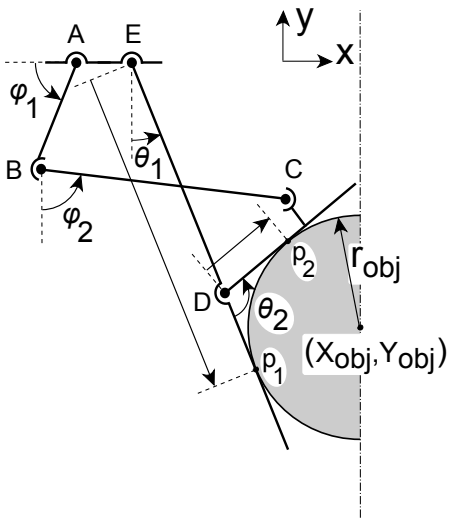

Figure 7: Schematic with; gripper angles that describe the configuration of the CE (θ_1 and θ_2) and the configuration of the actuation mechanism (ϕ_1 and ϕ_2), contact points p_1 and p_2, and gripper joints.

We can also rewrite the loop closure vector equations such that we obtain an expression for the contact point p_1 and p_2,

$$p_1 = \frac{Y_{obj} - r_{obj}\sin\theta_1}{-\cos\theta_1} \tag{6}$$

$$p_2 = \frac{Y_{obj} + r_{obj}\sin(\theta_1+\theta_2) + L_2\cos\theta_1}{-\cos(\theta_1+\theta_2)} \tag{7}$$

Configuration of the actuation mechanism:

The configuration of the actuation mechanism can be described by the angles ϕ_1 and ϕ_2 (see Fig. 7), which are dependent of θ_1 and θ_2. An expression for ϕ_1 and ϕ_2 is obtained by using trigonometric equations (see Appendix C).

$$\phi_1 = \pi - arccos\left(\frac{{d_2}^2-{d_3}^2-{L_8}^2}{-2d_3L_8}\right) - arccos\left(\frac{{L_5}^2-{d_3}^2-{L_6}^2}{-2d_3L_6}\right) \tag{8}$$

$$\phi_2 = \frac{\pi}{2} - arccos\left(\frac{{d_3}^2-{L_5}^2-{L_6}^2}{-2L_5L_6}\right) + \phi_1 \tag{9}$$

where d_2 is the distance between joint C and E, d_3 is the distance between joint A and C (see Fig. 7).

3.2 Dimensioning design parameters

To be able to examine the proper working of the gripper mechanism, we need to dimension the design parameter set S (see Eq. 1). In this section we will manually select proper values for the design parameters. To be able to do this, we will first examine the boundary conditions that we need to adhere to. In Sect. 3.2.1 the important elements for a proper dimensioning of the CE are discussed. In Sect. 3.2.2 the important elements for a proper dimensioning of the actuation mechanism are discussed. Section 3.2.3 presents a set of design parameters that can be used to examine the proper working of the gripper mechanism.

3.2.1 Boundaries on connecting elements

The CE are parameterised by the design parameters L_0, L_1, L_2 and L_4 (see Fig. 6a). The following relations between the CE and object size form boundary conditions for the dimensioning of the design parameters.

Gripper width and object size:
To make sure the object is in force equilibrium, the summation of all horizontal force components and the summation of all vertical force components active on the object, should both be zero. This means that each force applied onto the object, should have an opposing force component of the same magnitude. Looking at circular objects, this means a contact point should have or an exactly opposing contact point, or on each side a contact point that is positioned more than 90 degrees and less than 180 degrees apart. For frictionless contact points, this means that the maximum object size is determined by the design parameter L_0. When the radius of the object is larger than L_0, the contact points on the left and right LCE are spread more than 180 degrees apart. This means that force equilibrium is not possible and the object will always be ejected. This leads to the following upper bound on the object size,

$$r_{obj} < L_0 \tag{10}$$

LCE length and object size:
A grasping sequence starts by positioned the gripper over the object in a full open state, i.e. $\theta_1 = 0$. The distance between the base of the gripper and the ground surface is determined by the length of the LCE. The base of the gripper should not interfere with the product, which leads to a second upper bound on the object size,

$$r_{obj} < \frac{L_1}{2} \tag{11}$$

Joint position and object size:
For the grasp to exist, both the LCE and UCE should be able to make contact with the object. The UCE can only make contact with the object if the contact point on the LCE fulfills the following condition, $L_2 < p_{1,k} < L_1$. This can be translated to a third upper bound on the object size,

$$r_{obj} < L_1 - L_2 \tag{12}$$

Ratio LCE length and object width:
The LCE should be long enough to be able to make contact with the lower half of the object, i.e. LCE and object are tangent to each other. The combination of minimal object size and LCE length (L_1), gives an upper limit on the gripper width (L_0),

$$L_0 \leq L_1 \sin\theta_{1,c} + r_{min}\cos\theta_{1,c} \tag{13}$$

with $\theta_{1,c}$ the angle of the LCE when in contact with the object,

$$\theta_{1,c} = \arccos\left(\frac{r_{min} - L_1}{\sqrt{{r_{min}}^2 + (-L_1)^2}}\right) + \arctan\left(\frac{r_{min}}{-L_1}\right) \tag{14}$$

and where r_{min} is the minimum object size. Figure 8 shows, that when the gripper width and LCE length are known, Eq. (13) can be interpreted as a lower bound on the object size.

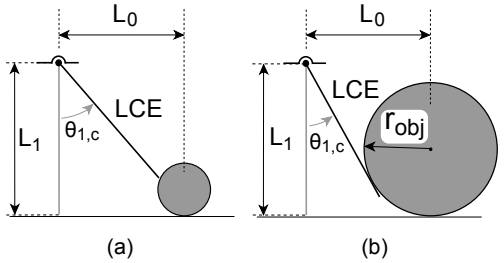

Figure 8: L_0 and L_1 represent the gripper width and LCE length, respectively. The angle of the LCE when in contact with the object is denoted by $\theta_{1,c}$ (a) Gripper configuration where object is too small for the LCE to make contact with the object. (b) Gripper configuration and object size that results in a proper contact by the LCE.

LCE and UCE length:
Since only cylindrical objects are considered and for a successful grasp the CE should be tangent to the object, the contact points p_1 and p_2 are equally distanced from joint D (see Fig. 7). Therefore, the UCE should be the same size as the part of the LCE where the object can make contact with,

$$L_4 = L_1 - L_2 \tag{15}$$

3.2.2 Boundaries on actuation mechanism

The actuation mechanism is parameterised by the design parameters L_3, L_5, L_6, L_7 and L_8 (see Fig. 6b). These design parameters should be chosen such, that they do not limit the desired grasp range. A bad dimensioning can limit the opening range or closing range of the gripper. An example of a limitation on the closing motion can be seen in Fig. 9a. Here, the maximum closing motion is limited by linkage L_5 and L_6 that are in line with each other and have reached the maximum distance between base joint and LCE connection. An example of a limitation on the opening motion can be seen in Fig. 9b. Again, the maximum closing motion is limited by linkage L_5 and L_6 that are in line with each other, but now the minimal distance between base joint and LCE connection has been reached.

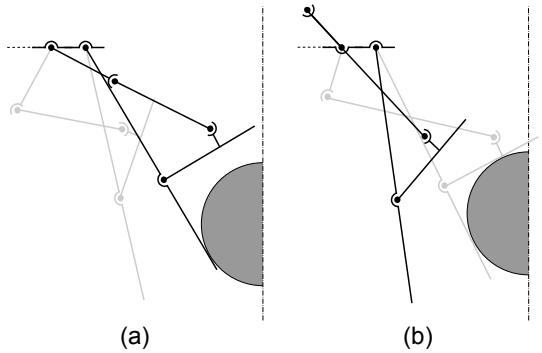

Figure 9: (a) Limitation on closing motion of gripper by actuation mechanism. (b) Limitation on opening motion of gripper by actuation mechanism.

3.2.3 Design parameter set

Sections 3.2.1 and 3.2.2 show that for a proper dimensioning of the design parameters, a desired object range is required. To evaluate the gripper mechanism, we introduce a similar object range as was used for the evaluation of the Delft Hand 2 [9]. The gripper mechanism is dimensioned for objects ranging from 60mm to 120mm diameter. To assist in the selection of proper values for the design parameters, a graphical users interface (GUI) is constructed (see Appendix E). Using the GUI and the boundary conditions described in the previous sections, manually a set of design parameters (S_1, see Table 1) is selected. Due to the many design parameters and intertwined relations, the calculation of a set of design parameters that results in a feasible grasp configuration is a complex task. Therefore a trial and error method is used by selecting the design parameters manually using the GUI. The selected design parameter set S_1, has at least one known object size for which force equilibrium of object and gripper exists.

Table 1: Dimensions of the design parameters set S_1, used for the analysis. See Fig. 6 for the design parameters.

Parameters	L_0	L_1	L_2	L_3	L_4	L_5	L_6	L_7	L_8
Size [mm]	80	130	60	40	50	60	50	2	10

3.3 Force equilibrium

A key question is whether the gripper mechanism can establish a final stable grasp for the complete object range without moving any object. To answer this question, this section presents a simple force analysis, discusses some grasp configurations that should be avoided and discusses the effects of non-cylindrical objects.

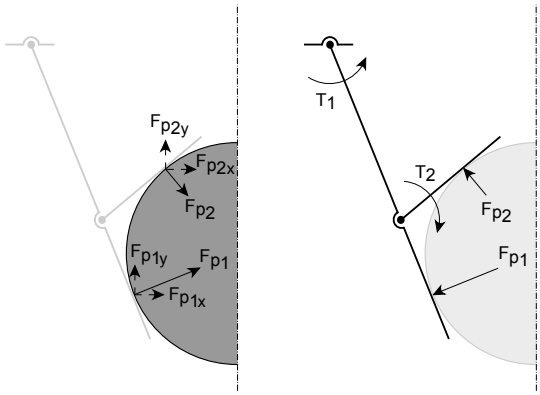

Figure 10: (a) Force components from the contact forces by the CE. (b) Representative torques T_1 and T_2.

For the force analysis, we make use of the actual applied contact force by the CE and the required contact force for force equilibrium. The following steps are followed. First we determine the configuration of the CE using Eqs. 4 and 5. Then the required contact force is determined and finally the actual applied force is determined. For force equilibrium to exist, the applied en required contact force should be equal.

Required contact force:
Since a cylindrical object in the centre of the gripper is assumed, only vertical force components applied on the object are of interest. For force equilibrium at initial contact the following should apply to the situation (see Fig. 10a),

$$F_{p1_y} + F_{p2_y} = 0 \tag{16}$$

To eliminate the magnitude of the actuation torque, we use the ratio of the applied forces by the LCE and UCE. The ratio (R_{req}) gives an expression for the relation between the forces exerted by the LCE and UCE that are required for force equilibrium,

$$R_{req} = \frac{F_{p_2}}{F_{p_1}} = \frac{\sin(\theta_1)}{\sin(\theta_1 + \theta_2)} \tag{17}$$

Applied contact force:
Using free body diagrams, the force within the complete system (configuration of the CE and actuation mechanism) is examined (see Appendix D). From this analysis the actual applied forces by the LCE and UCE are determined and an expression for the ratio of the applied normal forces ($R_{applied}$) is obtained.

Figure 11 shows R_{req} and $R_{applied}$ for the given object size range and the given design parameter set S_1 (see Table 1). The figure shows that for the given set of design parameters, only one object size achieves force equilibrium at initial contact. Several sets of parameters have been analysed and it turns out that each set of parameters only has one corresponding object size that results in force equilibrium at initial contact. All other object sizes in the given object size range, can not be grasped without moving the object.

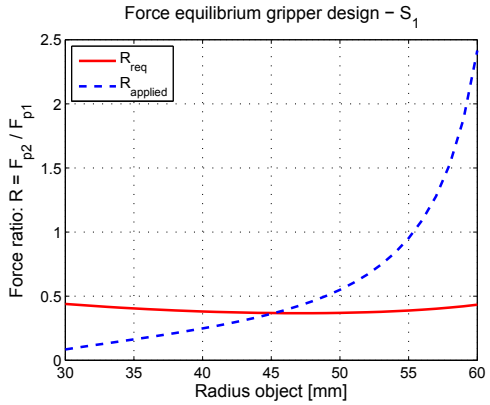

Figure 11: Graph with required (R_{req}) and applied ($R_{applied}$) force ratios for object sizes ranging from 60 mm to 120 mm diameter. The gripper is dimensioned with the design parameter set S_1. When R_{req} and $R_{applied}$ have the same force ratio, the gripper can establish force equilibrium of object and gripper at initial contact.

During the force analysis, several grasp configurations are encountered that required a pulling force by the object on the LCE or UCE to achieve force equilibrium of the gripper. This occurs when the distribution of the actuation force results in a negative torque on the respective CE. These configurations should be avoided since force equilibrium of object and gripper will never be possible.

Negative torque on LCE:
A negative torque on the LCE is caused by the UCE that pushes the LCE away from the object. These situations can be recognized as follows. There are three points at the UCE where forces are exchanged with other elements:

- Joint C, actuation forces transmitted by bar BC, line of action in the direction of bar BC (see Fig. 12).

- Contact point p_2, reaction force from object, line of action perpendicular to UCE.
- Joint D, reaction forces from LCE.

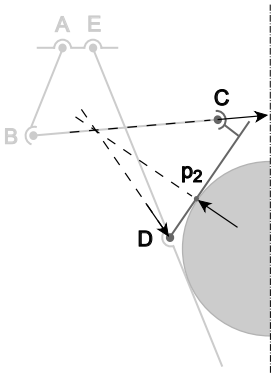

Figure 12: Grasp configuration where the common point of the concurrent forces is positioned on the left side of the LCE. Consequently, no force equilibrium of object and gripper is possible.

For the UCE to be in total equilibrium and at rest, the three external forces should be concurrent. When the common point of the concurrent forces is positioned on the left side of the LCE, the reaction forces at joint D create a negative torque on the LCE. The common point of the concurrent forces is always at the intersection of bar BC and a line perpendicular to the contact point p_2.

Negative torque on the UCE:
A negative torque on the UCE is caused by the actuation bar BC that pulls the UCE away from the object. This situation only occurs when in a grasp configuration linkage BC, or an extension of the linkage in the direction of joint B, crosses the UCE (see Fig. 13).

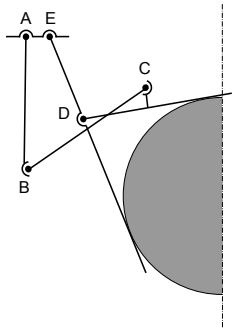

Figure 13: Improper gripper configuration. The gripper configuration results in a pulling force by the actuation mechanism on the UCE. Consequently, no force equilibrium of object and gripper is possible.

When we look at non-cylindrical objects, a short analysis quickly reveals that shape varying objects result in a force equilibrium problem for underactuated grippers. Two objects can be grasped that require a similar configuration of the CE, but have different contact points on the LCE and/or UCE (see Fig. 14). When the configuration of the CE does not change, i.e. θ_1 and θ_2 do not change, equation (17) shows that the required force ratio (R_{req}) stays unchanged. The required force ratio does not depend on the actual contact location p_1 and p_2 on the LCE and UCE. However, the actuation system distributes the actuation force over the LCE and UCE. How this actuation force is distributed depends on the configuration of the actuation mechanism, this counts for any underactuated gripper mechanism. The distributed actuation force can be represented by a torque T_1 and T_2 applied on the LCE and UCE, respectively (see Fig. 10b). These torques are responsible for the applied normal forces by the LCE and UCE, this means the actual applied forces by the LCE and UCE onto the object do depend on the contact points p_1 and p_2. In the situation sketched in Fig. 14, it shows that only the contact point on the LCE changes. Since the configuration of the CE does not change, the configuration of the actuation mechanism does not change either, consequently the representative torques T_1 and T_2 remain unchanged. The required force ratio is for both situations the same, but due to the different contact point p_2, the actual applied torque ratios differ. This shows that for any set of design parameters, there will always be objects for which force equilibrium at initial contact can not be established.

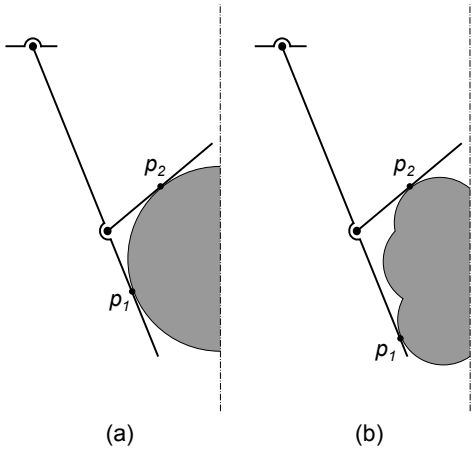

Figure 14: Two situations where the configuration of the CE is similar, but different contact points between object and LCE (p_1). Since for both situations the actuation force is the same, force equilibrium of object and gripper is not possible for these situations both.

3.4 Grasp stability

When force equilibrium of gripper and object is achieved, it is important that the gripper configuration is a stable configuration. When the object is slightly moved with respect to the gripper, an unstable configuration can result in a loss of the object. Therefore, it is important to look at the grasp stability of the gripper. A grasp is stable when a successful grasp (i.e. force equilibrium of object and gripper is established) returns towards its equilibrium point after a position disturbance. The stability of the gripper is investigated by examining the force ratios (see Sect. 3.3).

Figure 15 shows a graph of the required and applied force ratios for different y-position of the object. The used design parameters of the gripper can be found in Table 1. The object size used, is an object diameter of 90mm. The graph shows there is force equilibrium when the centre of the object is located about 84mm below the base of the gripper. When the object is located further below the base of the gripper, the applied force ratio is lower than the required force ratio. A lower applied force ratio means that the force applied by the UCE is too low with respect to the

force applied at the LCE to achieve force equilibrium. In other words, the magnitude of the vertical force component applied by the UCE is lower than the magnitude of the vertical force component applied by the LCE, this results in an upwards motion of the object. When the applied force ratio is higher than the required force ratio, a similar reasoning can be made and it shows that the object will start a downwards motion. Thus, for stability we require that for positions above the equilibrium point, the applied force ratio should be be larger than the required force ratio; the applied force ratio should be smaller than the required force ratio for positions below the equilibrium point. From this, we can be conclude that the shown grasp configuration is stable.

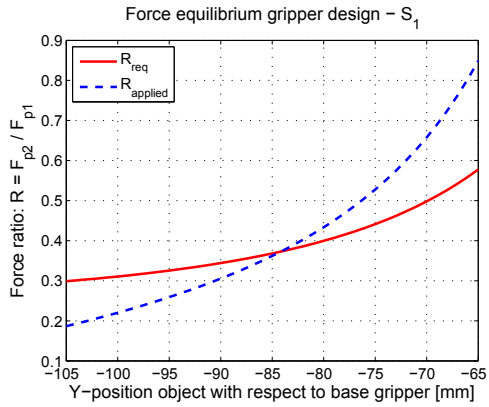

Figure 15: Graph with required and applied force ratios for different vertical positions of object with respect to the gripper. The gripper is dimensioned with the design parameter set S_1, and the object has a radius $r_{obj} = 45$mm.

3.5 conclusion

The study shows that without contact friction, the presented gripper can only achieve a final and stable grasp without moving the object, when the gripper mechanism is specifically designed for this object. This means, that without contact friction the gripper can not handle a range of products that vary in shape and size. In fact, we can conclude from this study that for a range of products that vary in shape and size, no underactuated gripper mechanism can be designed that is able to establish a final and stable grasp without moving the object (provided that all CE are part of the underactuated system).

4 Model including friction

In this section, we add static contact friction to the gripper model. The goal of this section is to investigate whether static contact friction has a positive influence on the grasp behavior or not. It is important to keep in mind that the design should not be made to rely on friction force. Although the previous chapter has shown that friction force is a necessity for achieving an instant stable grasp for a wide range of products, friction force should still be limited to avoid excessive damage. To expand our research, we will also study the effects of horizontal object displacement and gravity on the grasp behavior.

In Sect. 4.1 we define a new method, which includes contact friction, to determine the possibility of force equilibrium of object and gripper. This method is used in Sect. 4.2 to study the effects of changing object parameters on force equilibrium. Section 4.3 describes the effects of contact friction on the grasp stability. Section 4.4 describes the influence of mass and actuation torque on the grasp behavior. In Sect. 4.5 we address the possibility of grasping non-cylindrical objects.

4.1 Force equilibrium determination

Due to the addition of static contact friction to the model and the possibility of horizontal displacement of the object, force equilibrium can not be determined anymore as in Sect. 3.3. Therefore, we will now describe an alternative method to determine force equilibrium of object and gripper.

Due to the horizontal object displacements, we will encounter asymmetric grasp configurations. Therefore, the full gripper needs to be modeled now. The contact points on the LCE and UCE of the right half of the gripper are named, p_3 and p_4 respectively. From now on, the normal forces at the contact points p_i, with $i \in \{1,2,3,4\}$, are referred to as F_{pi_N}, with $i \in \{1,2,3,4\}$. Since static contact friction is taken into consideration, four variables (F_{pi_t}, $i \in \{1,2,3,4\}$) are added to the equilibrium equations (see Appendix F). The complete model of the gripper including object, comprises 27 equilibrium equations and 28 variables. This means the system is under determined and there are multiple solutions to solve this system. When we examine the equilibrium equations (Appendix F), we see that the normal force at contact point 2 and 4 are directly determined by the configuration and design parameters of the system. The normal force at contact point 1 and 3, and the friction force, are related and dependent of each other. The friction force at a contact point is bound by the static friction model,

$$-\mu F_{pi_N} \leq F_{pi_t} \leq \mu F_{pi_N}, \quad i \in \{1,2,3,4\} \tag{18}$$

where, μ is the static friction coefficient, F_{pi_N} is the normal force and F_{pi_t} is the friction force at contact point *i*. These inequality constraints limit the solution space of the system. In some situations the solution space is limited in such a way that there is no feasible solution available anymore. This means that in this specific situation there is no grasp stability at initial contact possible. Therefore, we define a possible force equilibrium at initial contact as the existence of at least one set of solutions that adheres both the equilibrium conditions of gripper and object, and the inequality constraints on the friction forces.

To check whether force equilibrium is possible or not, we need to look at the inequality constraints (Eq. 18). As already mentioned, the normal forces at contact points 2 and 4 are determined by the configuration of the gripper and the design parameters. For a given situation we can calculate these normal forces. Using the equilibrium equations (Eqs. F.1 - F.15), the dependent normal force and the friction force (F_{p1_N}, F_{p1_t}, F_{p3_N}, F_{p3_t} and F_{p4_t}) can be written as functions of F_{p2_t}. This means that the inequality constraints can be rewritten in the following form,

$$\begin{array}{rcccl} c_1 & \leq & F_{p2_t} & \leq & c_2 \\ -\mu.f(F_{p2_t})_1 & \leq & f(F_{p2_t})_2 & \leq & \mu.f(F_{p2_t})_1 \\ -\mu.f(F_{p2_t})_3 & \leq & f(F_{p2_t})_4 & \leq & \mu.f(F_{p2_t})_3 \\ c_3 & \leq & f(F_{p2_t})_5 & \leq & c_4 \end{array} \tag{19}$$

where, $f(F_{p2_t})_i$, $i \in \{1, 2, \ldots, 5\}$ are linear functions and c_i, $i \in \{1, 2, 3, 4\}$ are known constants for a given configuration and parameter set. For each inequality constraint in (19),we can now determine the lower and upper bound of the domain of F_{p2_t}. If and only if the following holds,

$$\{L_{b,1}, L_{b,2}, L_{b,3}, L_{b,4}\} \leq \{U_{b,1}, U_{b,2}, U_{b,3}, U_{b,4}\} \quad (20)$$

where, $L_{b,i}$ and $U_{b,i}$ are respectively the lower and upper bound of the *i*-th inequality constraint (Eq. 19), there is force equilibrium possible at initial contact. The feasible domain of F_{p2_t}, is the part of the domain of F_{p2_t} for which Eq. 20 holds.

4.2 Force equilibrium

Using the method described in the previous section, we can now study the effects of changing object and design parameters on force equilibrium configurations. In Sect. 4.2.1 we examine the influence of changing object parameters. Section 4.2.2 describes the effect of changing design parameters.

4.2.1 Varying object parameters

For a gripper with design parameter set S_1 (see Table 1), we examine the feasible grasp range. The feasible grasp range is here defined as the configurations of object and gripper, for which force equilibrium at initial contact can be established without moving the object. With configurations of object and gripper, we mean various object sizes and horizontal displacements of the object with respect to the gripper. Figure 16 shows the resulting force applied onto the object for a range of object sizes. The object is laying on a surface and is positioned in the centre of the gripper. The resulting force shown, is normalised by the actuation torque that is applied by the actuator. When the resulting force is zero, it means force equilibrium at initial contact is possible. The value of a non-zero normalized resulting force does not necessarily represent the actual resulting force onto the object, it merely shows force equilibrium at initial contact is not possible. The gripper model is analysed for three different static friction coefficients ($\mu \in \{0.1, 0.2, 0.3\}$). Figure 17 also shows the normalized resulting force for these three models, but here a constant object radius ($r_{obj} = 45$mm) and a varying horizontal displacement are used.

From Sect. 3, we concluded that the gripper mechanism with frictionless contact points could only establish force equilibrium at initial contact for one specific object. Figures 16 and 17 show that with contact friction, the gripper mechanism can establish force equilibrium at initial contact for multiple configurations, i.e. various object sizes and horizontal displacements of the object. The figures also show that an increase of the coefficient of friction results in an increase of the feasible grasp range. We can explain the latter finding as follows. A larger coefficient of friction results in larger possible friction force when the applied normal force stays the same, a larger friction force allows the object to be better constrained and therefore force equilibrium at initial contact for more configurations can be established. The friction force compensates for the unbalance created by the normal forces that is applied by the LCE and UCE. However, a larger friction force can result in more product damage. Each product has a limit of tolerable shear force, before it gets damaged. Increasing the coefficient of friction, e.g. by using different materials on the LCE and UCE, until the desired feasible grasp range is achieved, is therefore not an option.

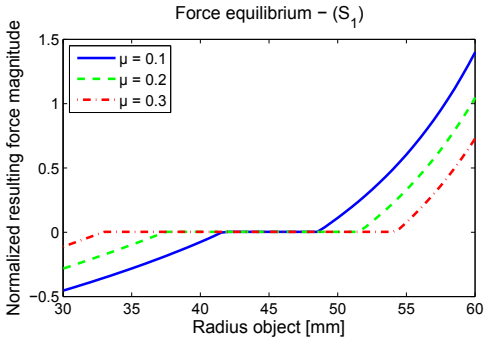

Figure 16: Normalised resulting force active on an object positioned in the centre of a gripper with design parameter set S_1 for varying object size.

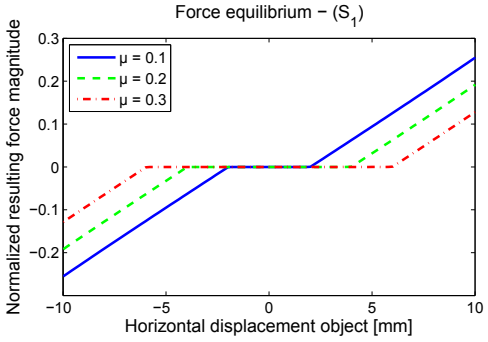

Figure 17: Normalised resulting force active on an object for varying horizontal displacements. A gripper with design parameter set S_1 is used and the object has a radius of $r_{obj} = 45$mm.

4.2.2 Varying design parameters

Figures 18 and 19 show the effect of a different dimensioning of the design parameters. We use the design parameter set S_1 and S_2 (see Table 2). For both models a static coefficient of friction of 0.2 is used. The figures shows that a slight alteration of the design parameters, only design parameters L_3 and L_7 are altered, result in a large effect on the feasible grasp range. With respect to object size, it can be concluded that design parameter set S_2 has a larger feasible grasp range. However, the maximum object size for which force equilibrium at initial contact can be established, is lower. Design parameter set S_2 also has a larger feasible grasp range when it comes to horizontal displacements of the object. These results show that the design parameters have a large influence on the behavior of the gripper. However, the mechanism is too complex to determine the effect each single design parameter has on the grasp behavior.

Table 2: Dimensions of the design parameters set S_2. See Fig. 6 for the parameters.

Parameters	L_0	L_1	L_2	L_3	L_4	L_5	L_6	L_7	L_8
Size [mm]	80	130	60	45	50	60	50	10	10

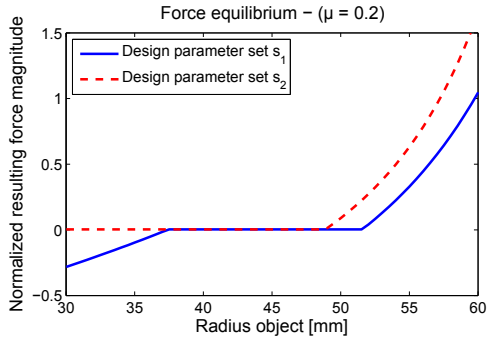

Figure 18: Normalised resulting force active on an object positioned in the centre of the gripper for a varying object size. Two different design parameter sets are used.

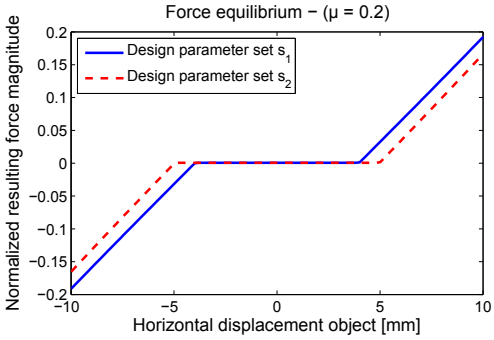

Figure 19: Normalised resulting force active on an object for varying horizontal displacements. A friction coefficient of $\mu = 0.2$ is used and the object has a radius of $r_{object} = 45$mm.

4.3 Grasp stability

The former stated definition on grasp stability, i.e. after a disturbance the object will return to its equilibrium position again, does not hold anymore now friction is taken into consideration. The new system has multiple configurations for which force equilibrium exists, as shown in the previous section. When an object is grasped and force equilibrium at initial contact is established, a large enough disturbance will still be able to move the object with respect to the gripper. However, when the disturbance is eliminated or extinguishes, the new acquired configuration might be an equilibrium configuration as well, consequently the object will not return to its initial equilibrium position. Therefore, we state that stability of the system is of less importance since a larger feasible grasp range is created.

4.4 Influence object mass and actuation force

We will now describe how the actuation torque can maintain force equilibrium while the object mass increases. This is done by examining a situation where we use, a fixed set design parameters, a fixed coefficient of friction, a fixed object size and horizontal displacement, only the object mass and actuation force will be changed. The analysis starts with a massless object and a feasible grasp configuration. For a given actuation torque, the independent contact forces F_{p2_N} and F_{p4_N} can be calculated (as is discusses in Sect. 4.1). The dependent contact forces F_{p1_N}, F_{p1_t}, F_{p2_t}, F_{p3_N}, F_{p3_t} and F_{p4_t} are such that force equilibrium of object and gripper exists and are each within their own bounds. Now the system will be disturbed by adding mass to the object. This will add a vertical force component to the object, which is directed downwards. Since the configuration of the gripper and actuation force will not change, the additional vertical force component has to be equilibrated by the dependent contact forces to maintain force equilibrium of object and gripper. The dependent contact forces F_{p1_t} and F_{p3_t} can help equilibrating the additional vertical force component, until they have reached their upper bound, i.e. $F_{pi_t} \leq \mu F_{pi_N}$ with $i \in \{1, 3\}$. From Eq. F.12 it can be seen that for a fixed configuration and actuation force, the dependent contact forces F_{p1_N} and F_{p3_N} fully depend on the magnitude of F_{p2_t} and F_{p4_t} respectively. It also shows that the maximum values of F_{p1_N} and F_{p3_N} are reached when F_{p2_t} and F_{p4_t} are on their boundary values. The static friction model (see Eq. 18) shows, that the boundary values of F_{p2_t} and F_{p4_t} on its turn are determined by the independent contact forces F_{p2_N} and F_{p4_N} respectively, which are a constant in this situation. This means, that as long as the dependent contact forces F_{p2_t} and F_{p4_t} have not reached their bounds, the mass of the object can be increased and force equilibrium of object and gripper is maintained. When the dependent contact forces F_{p2_t} and F_{p4_t} have reached their bounds and the mass of the object is increased even more, force equilibrium can be maintained by increasing the actuation force. Increasing the actuation force will increase the magnitude of the independent contact forces F_{p2_N} and F_{p4_N}, and therefore also the bounds of the dependent contact forces F_{p2_t} and F_{p4_t} will be increased. However, when for a feasible grasp configuration with a massless object the dependent contact forces F_{p1_t}, F_{p2_t}, F_{p3_t} and F_{p4_t} are already on their bounds, adding object mass can never result in a grasp where object and gripper are in force equilibrium, not even when the actuation torque is increased.

Adding object mass can be seen as adding a vertical force disturbance. The reasoning used in this section is therefore valid for any type of disturbance force. As long as there is room for the dependent contact forces to compensate a very small disturbance force, any disturbance force can be compensated by increasing the actuation torque. When increasing the actuation torque it needs to be kept in mind that this will automatically allow larger friction forces in the system and increases the active normal forces. Both can result in product damage and this is actually what is tried to be prevented with this gripper design.

4.5 Asymmetric objects

So far, we have only discussed cylindrical objects. This is because the mathematical model described in this paper is fully based on cylindrical objects. However, the gripper should also be able to handle non-cylindrical and asymmetric objects. When asymmetric objects are grasped, the configuration of the left half of the gripper might be different from the configuration of the right half of the gripper. Consequently, both gripper sides will apply different forces onto the object. The normal forces will not be concentric and without contact friction, force equilibrium is not possible. When there is contact friction between gripper and object, there is a possibility force equilibrium exists. Of course, this is only possible when there is room within

the bounds of the dependent contact forces to achieve force equilibrium, as discussed in the previous section.

4.6 Conclusion

This study has shown that the possible grasp configurations for which force equilibrium at initial contact can be established, increase under the influence of friction. When the coefficient of friction is increased, the feasible grasp range increases as well.

The contact friction forces can be seen as variable compensation forces. Within their limits, the contact friction forces can compensate any external disturbance force and correct a force difference resulting from the applied normal forces between object and gripper. With respect to external disturbance forces, the room for compensation by the contact friction forces is increased by increasing the actuation force. Since the friction forces leave room to correct a force difference resulting from the applied normal forces between object and gripper, a larger feasible grasp range is created. This also means that when the object its position with respect to the gripper is disturbed, it might not return to its initial equilibrium position anymore. Grasp stability of the gripper becomes therefore less important.

It can be stated that contact friction has an overall positive effect on the grasp performance of the gripper. The actual grasp performance of a gripper on non-cylindrical and asymmetric objects when contact friction is present, should be examined by performing some experiments because the mathematical model used in this paper is only valid for cylindrical objects.

5 Parameter optimization

This section describes the optimisation of the design parameters. The goal is to achieve force equilibrium over the complete grasp range whilst using a coefficient of friction that is as low as possible. Also the active friction force during a grasp is compared to the friction force occurring when a precision grasp would be performed. Section 5.1 describes the design case that is used for the optimisation process. In this section also the assumptions and boundary conditions used for the optimisation are described. In Sect. 5.2 the optimisation process is described as well as a method how to determine the contact friction forces in the system. The results of the optimisation are shown in Sect. 5.3. In this section also the optimised gripper design is tested against a gripper that establishes a precision grasp. Finally, a discussion and conclusion follow in Sect. 5.4 and 5.5, respectively.

5.1 Design case

To optimise and evaluate the gripper design, we introduce the following design case. The gripper is optimised for the use in a distribution centre for fruits and vegetables. The gripper should be able to handle delicate products that range from 60mm to 120mm in diameter. The products might not be perfectly aligned with the gripper. Therefore, we introduce a maximum positioning error ($p_\triangle$) of $\pm 5\%$ of the maximum object diameter for the complete object size range. For the design case, this means a maximum horizontal displacement of $\pm$6mm. The horizontal displacement should also point out whether the optimised gripper is able to cope with asymmetric grasp configurations or not. The object size range and horizontal displacement form the total grasp range. Gunnarsson [4] concluded from a literature study on the effects of underactuated grippers and friction, that for fruits and vegetables with respect to a rubber, the static coefficient of friction is 0.4 ± 0.1. This is used as the upper limit on the possible coefficient of friction in the design case.

5.1.1 Boundary conditions

During the optimisation process of this design case, we need to adhere to the same boundary conditions as discussed in Sect. 3, i.e.

- Limitation on closing and opening motion of gripper by faulty design parameters (see Fig. 9).
- Only compressive forces between object and UCE can be realised (see Fig. 12).
- Only compressive forces between object and LCE can be realised (see Fig. 13).
- Maximum ratio gripper width and LCE length (see Fig. 8).

However, we have introduced a possible horizontal displacement of the object. Therefore, the relation between L_0 and L_1 as given in Eq. 13 is not valid anymore and needs to be redefined,

$$L_0 \leq L_1 \sin\theta_{1,c} + r_{min}\cos\theta_{1,c} - X_{max} \qquad (21)$$

For the presented design case, Fig. 20 shows the maximum gripper width (L_0) for a given LCE length (L_1).

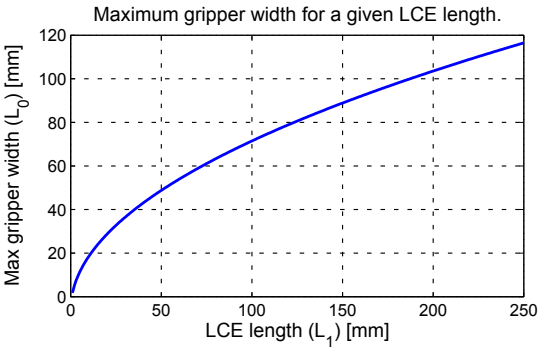

Figure 20: Graph that shows the maximum gripper width for a given LCE length for the design case. When a larger gripper width is chosen, the LCE can not make contact with the smallest object from the object range anymore. The minimum object size is 60mm diameter.

5.1.2 Design Assumptions

The optimisation will use the model described in Sect. 3 and 4. Therefore, we have to use the same design assumptions as made in Sect. 3 and 4, i.e.

- All elements of the gripper have zero thickness and infinite stiffness.
- The objects are modeled as cylindrical objects.

For the design case the following assumptions are added,

Spring forces:

The springs positioned between the LCE and UCE that ensure first contact is made with the LCE and subsequently with the UCE, can be positioned such that the spring force is neglectable compared to the other forces in the system when the gripper has made contact with the object. Therefore, for the design case we neglect the spring force.

Object mass:

1) To determine the minimum coefficient of friction, we use massless objects. With massless objects, the gripper and object can be seen as one system without external forces.
2) To be able to compare the friction forces occurring with the new gripper design and a gripper that performs a precision grasp, we add mass to the object. For the design case, the smallest object from the object range, i.e. $r_{min} = 30$mm, has a mass of $m = 0.085$kg. The mass of the object is related to the size of the object. This means the largest object from the object range, i.e. $r_{max} = 60$mm, has a mass of $m = 0.340$kg.

Actuation torque

1) To determine the minimum coefficient of friction, actuation is of no importance. Since there are no external forces, the magnitude of the actuation torque has no influence on the result of the optimisation process.
2) For the comparison of the friction force between the new gripper design and a gripper that establishes a precision grasp, the actuation force is very important. The outcome of the optimisation process will be influenced heavily by the amount of actuation force. Therefore, the optimisation will be performed with a range of actuation torques, i.e. $T_a \in \{600, 800, \ldots, 1600\}$Nmm.

5.2 Method

Section 5.2.1 describes the method that is used to optimise the design parameters such that we obtain the minimum coefficient of friction for which a complete feasible grasp range is possible. Section 5.2.2 describes the method that is used to determine the required contact friction force for force equilibrium of gripper and object.

5.2.1 Optimisation

For the optimisation, two steps are required. The optimisation starts with a coefficient of friction of 0.4. Step one is to optimise the design parameters such that a complete feasible grasp range is possible for the given coefficient of friction. When this is possible, the second step is to lower the coefficient of friction. These steps are repeated until no complete feasible grasp range can be achieved anymore.

For step one, a performance indicator is needed that represents the performance of a gripper with a given set design parameters S. The feasible grasp range compared to the total grasp range is used as the performance indicator. The performance indicator (Q) can be expressed as follows,

$$Q(S) = \frac{\sum_{j=1}^{b}\sum_{i=1}^{a} Z\left(r_{obj_i}, X_{obj_j}, S\right)}{a.b} \tag{22}$$

with,

$$a = \frac{r_{max} - r_{min}}{\Delta r} + 1$$

$$b = \frac{4.p_\Delta.r_{max}}{\Delta X} + 1$$

where, r_{min} and r_{max} are respectively the minimum and maximum radius of the object, Δr is the step size of object diameter in the grasp range, ΔX is the step size of horizontal object displacement in the grasp range, p_Δ is the percentage used to determine the maximum horizontal displacement, and $Z\left(r_{obj_i}, X_{obj_j}, S\right)$ is the grasp feasibility factor for the i-th object size and j-th horizontal displacement location. The value of $Z\left(r_{obj_i}, X_{obj_j}, S\right)$ is determined according the following rule,

if, (an impossible grasp configuration is created due to the selected design parameter set S),
$Z\left(r_{obj_i}, X_{obj_j}, S\right) = -0.01$
elseif, (there exists force equilibrium for design parameter set S, r_{obj_i} and X_{obj_j}),
$Z\left(r_{obj_i}, X_{obj_j}, S\right) = 1$
else,
$Z\left(r_{obj_i}, X_{obj_j}, S\right) = 0$

where,

$$r_{obj_i} \in \{r_{min}, r_{min} + \Delta r, \ldots, r_{max}\}$$

$$X_{obj_j} \in \{-2.p_\Delta.r_{max}, -2.p_\Delta.r_{max} + \Delta X, \ldots, 2.p_\Delta.r_{max}\}$$

and together represent the complete grasp range. With *an impossible grasp configuration* we mean configurations where not all CE can make contact with the object, or configurations where a pulling force is required by a CE to establish force equilibrium of object and gripper. The method described in Sect. 4.1, is used to determine whether force equilibrium is possible or not. A performance indicator of $Q = 1$ represents a complete feasible grasp range. A lower value of Q shows that for the given set of design parameters, there exist grasp configurations in the complete grasp range where force equilibrium of object and gripper can not be established. For the optimisation used in the design case, Δr and ΔX are 1.

The unconstraint nonlinear solver *fminsearch.m* in MATLAB is used to find a set of design parameters (S) that results in the maximum performance indicator (Q) for a given coefficient of friction. This solver uses the Nelder-Mead simplex direct search algorithm. For the optimisation, the design parameters L_3, L_5, L_6, L_7 and L_8 (see Fig. 6) are used as optimisation variables and the objective function is represented by,

$$\underset{S}{\text{minimize}} \quad -Q(S) \tag{23}$$

We use an unconstrained solver because the boundary conditions *Parameter length*, *Normal force UCE and LCE* (see Sect. 5.1.1) are already incorporated in the performance indicator, the boundary condition *Maximum ratio gripper width and LCE length* is too complex to incorporate in the optimisation. Adding design parameters L_0, L_1 and L_2 as variables to the objective function, would make the optimisation too complex and time consuming. Therefore, using the GUI we have selected some fixed values for these design parameters, which can be found in Table 3. When the minimum coefficient of friction is found for which still a

complete feasible grasp range can be achieved, we will analyse the influence of the fixed design parameters L_0, L_1 and L_2. When it shows that changing these design parameters could improve the performance indicator Q, the fixed design parameters are altered and the optimisation process is repeated again.

Table 3: Dimensions of the fixed design parameters L_0, L_1 and L_2 used in the optimisation for the design case.

Fixed design parameters	L_0	L_1	L_2
Size [mm]	103.5	200.0	50.0

The solution returned by the solver, might be a local minimum. Therefore, the solver is used with multiple initial starting values for the optimization variables. See Table 4 for a list with different sets of starting values. It is important to verify that the different sets of starting values do not result in *an impossible grasp configuration*. This is first manually verified with the GUI.

Table 4: Different sets with starting values used for the optimisation process in the design case.

Set	L_3 [mm]	L_5 [mm]	L_6[mm]	L_7 [mm]	L_8[mm]
1	10.0	35.0	30.0	20.0	10.0
2	10.0	50.0	45.0	25.0	20.0
3	20.0	70.0	20.0	15.0	10.0
4	20.0	50.0	40.0	25.0	25.0
5	30.0	50.0	40.0	25.0	10.0
6	30.0	70.0	25.0	15.0	20.0
7	40.0	80.0	20.0	15.0	15.0
8	40.0	90.0	30.0	30.0	25.0
9	50.0	90.0	25.0	30.0	10.0
10	50.0	100.0	15.0	15.0	20.0
11	60.0	90.0	25.0	10.0	5.0
12	60.0	110.0	15.0	25.0	20.0
13	70.0	100.0	30.0	25.0	10.0
14	70.0	120.0	15.0	30.0	15.0
15	80.0	110.0	35.0	30.0	15.0
16	80.0	130.0	25.0	40.0	25.0

5.2.2 Friction force determination

In the following section, the contact friction force at each contact point is determined and compared to the friction force at the contact points of a gripper that performs a precision grasp. We will now explain how to determine the possible friction forces in the system.

First we focus on a single grasp configuration out of the complete grasp range. For this grasp configuration the feasible domain of F_{p2_t} is determined (see Sect. 4.1). For the complete feasible domain (a step size of $\Delta = 0.01$ is used in the design case), the total magnitude of the contact friction force is calculated. The friction force at each individual contact point is registered for the value of F_{p2_t} that has the lowest total magnitude of the contact friction force. This process is repeated for the complete grasp range.

We assume that the gripper that establishes a precision grasp, is not negatively influenced by a horizontal displacement of the object. The precision gripper makes only two contact points with the object and the friction force is evenly distributed over these contact points. When comparing the active friction force of the two grippers, for the new design, we will use the maximum friction force at a contact point over the complete horizontal displacement range.

5.3 Results

In this section the results of the optimisation process are presented. In Sect. 5.3.1 the minimum required coefficient of friction for the design case without external forces is presented. In Sect. 5.3.2 object mass is taken into account and the minimum required friction forces of the optimised new gripper design are compared to the minimum required friction forces for a gripper that establishes a precision grasp.

5.3.1 Minimum coefficient of friction

For an extensive list with results from the optimisation process, see Appendix G.1.

Table 5: Two sets of design parameters from the optimisation process. Set 1 results in a complete feasible grasp range for the lowest possible coefficient of friction, i.e. $\mu = 0.06$. Set 2 results in the best performance indicator (Q) for a coefficient of friction of $\mu = 0.05$. The optimisation is performed for massless circular objects ranging from 60mm to 120mm diameter and a horizontal displacement of $\pm$6mm. The following fixed design parameters are used: $L_0 = 103.5$mm, $L_1 = 200.0$mm and $L_2 = 50.0$mm.

Set	μ	Q	L_3 [mm]	L_5 [mm]	L_6 [mm]	L_7 [mm]	L_8 [mm]
1	0.06	1.00	10.8	30.1	46.7	28.8	20.5
2	0.05	0.94	32.0	47.7	39.9	26.1	10.3

Using the fixed design parameters from Table 3 and the starting values from Table 4, the lowest coefficient of friction for which a complete feasible grasp range can be found is $\mu = 0.06$ (see Table 5). For the set design parameters that has the best performance indicator for a friction coefficient of $\mu = 0.05$ (see Table 5, Set 2), we will now study the influence of changing the fixed design parameters L_0, L_1 and L_2. For the results see Fig. 21. Note that only the effects of a decreasing value of L_0 and increasing value of L_1 can be investigated, this is due to the boundary conditions on gripper width and LCE length (see Sect. 5.1.1).

Table 6: Three sets of design parameters from the optimisation process. Set 1 and 2 result in a complete feasible grasp range for the lowest possible coefficient of friction, i.e. $\mu = 0.05$. Set 3 results in the best performance indicator (Q) for a coefficient of friction of $\mu = 0.04$. The optimisation is performed for massless circular objects ranging from 60mm to 120mm diameter and a horizontal displacement of $\pm$6mm. The following fixed design parameters are used: $L_0 = 103.5$mm, $L_1 = 218.0$mm and $L_2 = 50.0$mm.

Set	μ	Q	L_3 [mm]	L_5 [mm]	L_6 [mm]	L_7 [mm]	L_8 [mm]
1	0.05	1.00	18.5	40.9	45.7	33.2	20.5
2	0.05	1.00	10.6	28.3	43.6	29.2	13.9
3	0.04	0.91	31.3	47.8	39.4	26.0	10.4

Figure 21 shows that increasing the design parameter L_1, can positively influence the performance indicator Q. Therefore, a new optimisation is performed for the fixed design parameters $L_0 = 103.5$mm, $L_1 = 218$mm and $L_2 = 50$mm. The initial starting values from Table 4 are used again. For an extensive list with results of the optimisation process, see Table G.2. There are two sets of design parameters found that result in a complete feasible grasp

range (see Table 6). For the set design parameters that has the best performance indicator for a friction coefficient of $\mu = 0.04$ (see Table 6, Set 3), we will now study the influence of changing the fixed design parameters L_0, L_1 and L_2. For the results see Fig. 22.

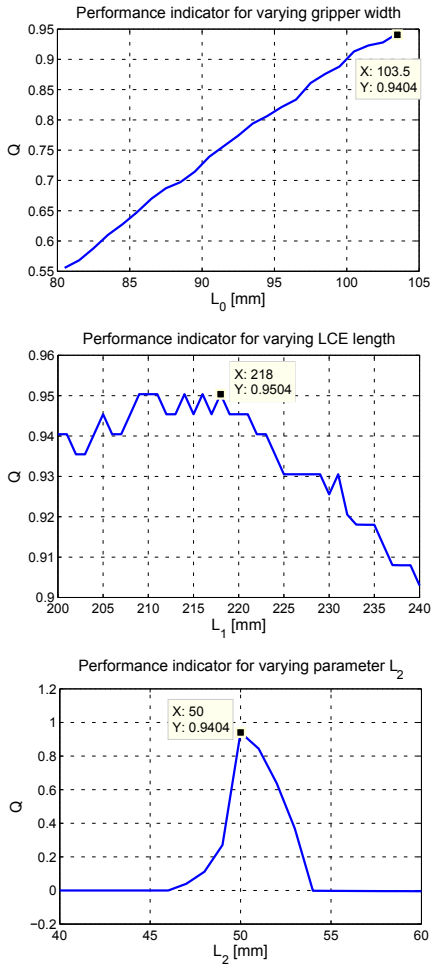

Figure 21: Three graphs that show the influence on the performance indicator Q when the fixed design parameters (L_0, L_1 and L_2) are altered. The design parameters used, can be found in Table 5 (Set 2).

Figure 22 shows that the performance indicator Q does not increase when the fixed design parameters are altered. However, an increase of L_1 for $L1 \in \{223, 227, 228\}$, shows equal behavior for the performance indicator. Since an increase of design parameter L_1 from 200mm to 218mm has already shown an improvement on the minimum possible coefficient of friction, we will perform a new optimisation with $L1 \in \{223, 227, 228\}$mm. The initial starting values from Table 4 are used again. For an extensive list with results of the optimisation process, see Table G.3. From the optimisation we obtain two sets of design parameters that result in a complete feasible grasp range for $\mu = 0.04$ (see Table 6, Set 1 and 2). Both sets involve a LCE length of $L_1 = 227$mm. The maximum performance indicator found for $\mu = 0.03$ with a LCE length of $L_1 = 227$mm is $Q = 0.88$ (see Table 6, Set 3). Analysis of the fixed design parameters of Set 3 from Table 6, has shown no improvement of the performance indicator Q.

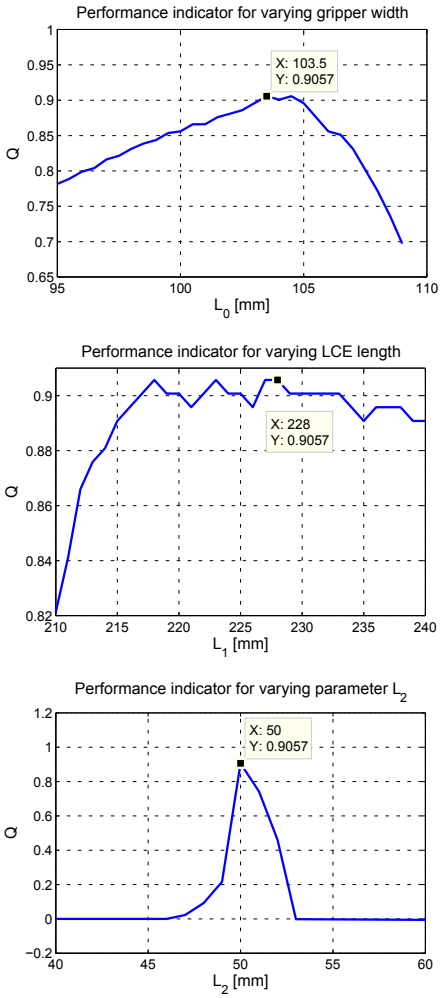

Figure 22: Three graphs that show the influence on the performance indicator Q when the fixed design parameters (L_0, L_1 and L_2) are altered. The design parameters used, can be found in Table 6 (Set 3).

Table 7: Three sets of design parameters from the optimisation process. Set 1 and 2 result in a complete feasible grasp range for the lowest possible coefficient of friction, i.e. $\mu = 0.04$. Set 3 results in the best performance indicator (Q) for a coefficient of friction of $\mu = 0.03$. The optimisation is performed for massless circular objects ranging from 60mm to 120mm diameter and a horizontal displacement of $\pm$6mm. The following fixed design parameters are used: $L_0 = 103.5$mm, $L_1 = 227.0$mm and $L_2 = 50.0$mm.

Set	μ	Q	L_3 [mm]	L_5 [mm]	L_6 [mm]	L_7 [mm]	L_8 [mm]
1	0.04	1.00	5.2	25.8	50.1	31.9	22.7
2	0.04	1.00	14.9	40.9	49.4	45.5	21.2
3	0.03	0.88	17.1	39.1	48.4	39.5	20.7

5.3.2 Minimum required friction forces

As stated in Sect. 5.1.2, object mass is added ranging from $0.085 - 0.340$kg, and the optimisation is performed for a range of actuation torques, i.e. $T_a \in \{600, 800, \ldots, 1600\}$. For an extensive list with results from the optimisation process, see Appendix H.1.

Using the fixed design parameters from Table 3 and the starting values from Table 4, the lowest coefficient of friction for which a complete feasible grasp range can be found

is $\mu = 0.09$ (see Table 8, Set 1). Altering the fixed design parameters L_0, L_1 and L_2, shows no improvement of the performance indicator Q for grasp configurations that do not have a complete feasible grasp range ($Q < 1.00$).

Table 8: The two sets of design parameters from the optimisation proces that result in a complete feasible grasp range and have the lowest total friction force (F_{p_t}). The optimisation is performed for circular objects ranging from 60mm to 120mm diameter and a horizontal displacement of ±6mm, the following fixed design parameters are used: $L_0 = 103.5$mm, $L_1 = 200.0$mm and $L_2 = 50.0$mm. Set 1 is the result from the optimisation with $T_a = 1400$Nmm and $\mu = 0.09$. Set 2 is the result from the optimisation with $T_a = 800$Nmm and $\mu = 0.2$.

Set	L_3 $[mm]$	L_5 $[mm]$	L_6 $[mm]$	L_7 $[mm]$	L_8 $[mm]$	$Total$ F_{p_t} $[N]$
1	13.3	23.0	55.7	28.2	20.3	1.817
2	32.6	37.7	49.5	23.7	9.9	2.161

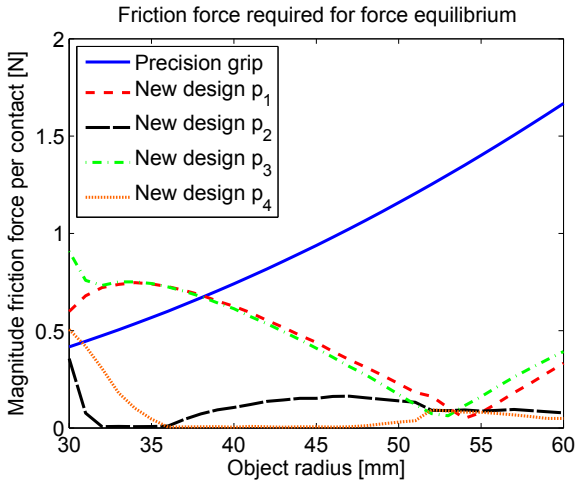

Figure 23: Graph with friction force at each contact point for the new gripper design and a gripper that performs a precision grasp, where p_1-p_4 are the contact points. The dimensions used for the new gripper design can be found in Table 8 (Set 1), the gripper works with a coefficient of friction of $\mu = 0.09$ and actuation torque of $T_a = 1400$Nmm.

The two sets with design parameters that result in the lowest total magnitude of friction force (see Table 8), are compared with a gripper that establishes a precision grasp. Figure 23 and 24 show the friction force at each contact point of the new gripper design and a gripper that performs a precision grasp for the complete object size range. For the new gripper design, the maximum friction values are shown of the various horizontal displacements.

5.4 Discussion

This section discusses the results of the optimisation. Section 5.4.1 gives an interpretation of the results from the optimisation process. In Sect. 5.4.2 the influence of the chosen parameters on the optimisation process are discussed. In Sect. 5.4.3 we give an interpretation on the results of the friction force in the system.

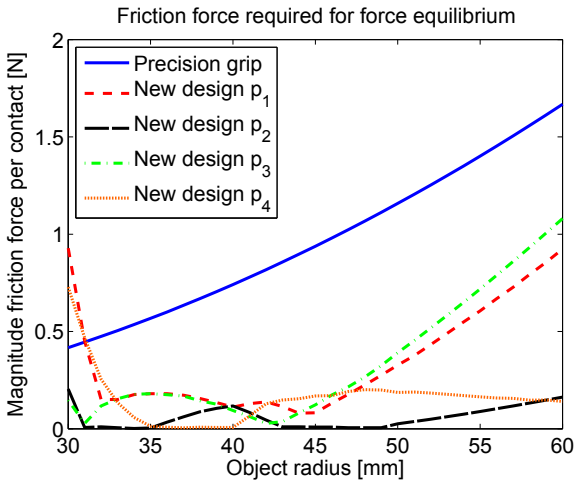

Figure 24: Graph with friction force at each contact point for the new gripper design and a gripper that performs a precision grasp, where p_1-p_4 are the contact points. The dimensions used for the new gripper design can be found in Table 8 (Set 2), the gripper works with a coefficient of friction of $\mu = 0.2$ and actuation torque of $T_a = 800$Nmm.

5.4.1 Interpretation of optimisation results

For the design case with massless objects (Sect. 5.3.1), the minimum coefficient of friction for which still a complete feasible grasp range can be obtained is $\mu = 0.04$. There are no external disturbing forces present in this design case. The only reason why friction force is required to establish force equilibrium of gripper and object, is because the normal force applied by the different CE do not equilibrate each other, but create an unbalance. However, the gripper design can be optimised such that this unbalance is very small, this is represented by the low coefficient of friction that is required for force equilibrium.

From Table 7 we see that two sets of design parameters with different dimensioning of the actuation mechanism, result both in a complete feasible grasp range. From the remaining results there is no obvious pattern that the optimisation converges to a single optimal gripper design. For each coefficient of friction the sets of design parameters that result in a complete feasible grasp range are different.

For the design case with object mass (Sect. 5.3.2), the minimum coefficient of friction for which still a complete feasible grasp range can be obtained is $\mu = 0.09$. For this optimisation the actuation torque is important since there is an external force active in the system, represented by the object mass. However, the actuation torque is not included as an optimisation variable, but as a parameter, i.e. $T_a \in \{600, 800, \ldots, 1600\}$. It is possible that with an actuation torque outside the specified range, a lower coefficient of friction is obtained for which still a complete feasible grasp range is possible.

5.4.2 Influence selected parameters

As initial parameters for the CE configuration, we have chosen to use the maximum ratio of gripper width to LCE length (see Fig. 8 and 20). When this maximum ratio is used, the LCE is better able to compensate vertical disturbance forces without relying on friction force. This can be

explained as follows. The maximum ratio of gripper width to LCE length, makes sure that the LCE is positioned under the largest possible angle θ_1 (see Fig. 25) when in contact with the object. This has as a result that the normal force applied by the LCE has a larger vertical force component than when the LCE is positioned under a smaller angle θ_1 (see Fig. 25). The optimisation where object mass is included (Sect. 5.3.2), indeed shows that decreasing L_0 or increasing L_1 has no positive influence on the performance indicator Q. However, for the design case where the minimum required coefficient of friction is determined (Sect. 5.3.1), the results show that an increase of the LCE length, and thus a decrease of the ratio of gripper width to LCE length, causes an improvement of the performance indicator. We believe this due to the exclusion of object mass or external forces.

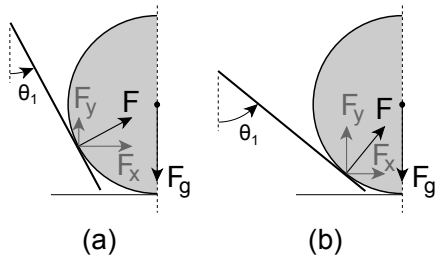

Figure 25: (a) Contact force for a small angle θ_1 of the LCE. (b) Contact force for a large angle θ_1 of the LCE.

The initial value of the fixed design parameter L_2, is chosen such that the configuration of the gripper does not change a lot when the object size changes or object position changes. When the configuration of the gripper does not change a lot, the forces in the system will not change much either. This increases the possibility of a complete feasible grasp range. However, changing the design parameter L_2, has a large influence on the total configuration of the gripper and therefore also on the grasp performance of the gripper. This is the reason why Figs. 21 and 22 show no improvement in performance indicator when L_2 is adjusted. A disadvantage from the optimisation method used, is that configurations with a different L_2 size are not explored.

5.4.3 Interpretation results on friction force

When looking at the results of the optimisation(see Appendix H.1), it shows that a lower coefficient of friction does not necessarily mean lower contact friction force in the system.

When we compare the two optimised gripper designs from Table 8 with a gripper that performs a precision grasp, Figs. 23 and 24 show that for the larger part of the object range, the contact friction force is lower in the systems of the optimised gripper designs compared to the gripper that performs a precision grasp. However, the figures also show that the two optimised gripper designs both have their own object range in which they perform best, i.e. a range where the contact friction force is minimal. The decision which gripper design to use, depends therefore on the frequency with which specific objects from the object range need to be handled. The figures also show that the largest friction force occur at the LCE (contact points p_1 and p_3).

5.5 Conclusion

The minimum coefficient of friction for which the optimised gripper design can still realise a complete feasible grasp range with massless objects, is $\mu = 0.04$. However, since not all design parameters are used as variables in the optimisation process, there might exist unexplored gripper parametrisations that result in an even lower possible coefficient of friction. The study has shown that when contact friction force is unwanted, the optimised gripper design outperforms a gripper that establishes a precision grasp.

6 Discussion

In this study we have designed an underactuated gripper mechanism that is able to establish a final grasp without moving the object. The gripper consists out of four rotating CE that allow the gripper to cope with shape and size variation of the object. A bar-linkage system is used to distribute the actuation forces over the CE. Section 6.1 discusses a simplification we introduced on the mathematical model and the optimisation method. Section 6.2 discusses a limitation on the design process and the optimisation method.

6.1 Simplifications

The mathematical model and therefore also the optimisation of the gripper design only comprise cylindrical objects. However, the gripper mechanism should also function with non-cylindrical objects. The horizontal object displacements used in the optimisation, make sure the gripper is able to handle asymmetric grasp configurations. Therefore, we assume that the gripper is also able to establish a final grasp without moving the object when objects are grasped that merely resemble cylindrical objects. The matter of how much an object needs to resemble a cylinder, depends on: (1) the maximum horizontal object displacement used in the optimisation process, (2) the amount of contact friction allowed between the object and gripper.

In this study we introduced elements with *zero thickness*. The assumption on *zero thickness* can be justified as follows. The CE can be made such that the part of the element that makes contact with the object is in line with the centre of the joints. This creates equal conditions to elements with zero thickness.

6.2 Limitations

The decision on the design of the actuation mechanism has been made without really considering other bar-linkage designs. The current design seemed to be the most simple design and was therefore assumed to be the best design. During the analysis of the gripper model including friction (Sect. 4), it was discovered that the actuation force of the LCE is influenced by the contact position of object and UCE. This results in several grasp configurations for which force equilibrium of object and gripper will not be possible (negative T_1, see Sect. 3.3). There exist configurations of the actuation mechanism that do not introduce faulty grasp configurations. However, these have not been looked into.

We have only performed a static analysis of the gripper mechanism while the gripper is designed for the pick and

place industry. When the gripper with object starts to move, the gripper mechanism will be subjected to large external disturbance forces. This study fails in giving insight into the dynamic aspect of the grasping process.

7 Conclusion

From this study we can conclude that:

- Using only movable CE, a gripper mechanism can be designed that can achieve a final stable grasp of an object without moving the object.
- To achieve a final stable grasp for an object range, i.e. various objects with different shape and/or size, there has to be contact friction present between object and gripper.
- The amount of contact friction needed to create a complete feasible grasp range is increased due to:
    1. Increase of variance of object size/shape for the object range.
    2. Increase of variance of object weight for the object range.
    3. Increase of magnitude of disturbing forces to be handled.

When the damage threshold, i.e. maximum amount of force an object can withstand without getting damaged, for a product is not known, no statement can be made whether this gripper mechanism will damage the product or not.

8 Future work

- Research the dynamic behavior of the gripper mechanism.
- The only way a gripper mechanism can be made that is able to establish a final stable grasp at initial contact without exploiting friction forces, is to create a form closed grasp around the object. Therefore, we advise to research the possibility to add one or multiple nonbackdrivable elements in the gripper design.

References

[1] A. Bicchi and V. Kumar. Robotic grasping and manipulation. 270:55–74, 2001.

[2] L. Birglen, T. Laliberté, and C. Gosselin. *Underactuated robotic hands*. Springer Verlag, 2008.

[3] C. Meijneke G. A. Kragten and J. L. Herder. An underactuated hand that mechanically converts between a power and precision grasp configuration. *The international journal of robotics research*, 2011.

[4] R.Ö. Gunnarsson. Underactuated grippers and friction. 2011.

[5] G. A. Kragten. Underactuated hands: fundamentals, performance analysis and design. 2011.

[6] S. Krut. A force-isotropic underactuated finger. In *Robotics and Automation, 2005. ICRA 2005. Proceedings of the 2005 IEEE International Conference on*, pages 2314–2319, 2006.

[7] X. Markenscoff, L. Ni, and C. H. Papadimitriou. The geometry of grasping. *The international journal of robotics research*, 9(1), 1990.

[8] B. Massa, S. Roccella, M. C. Carrozza, and P. Dario. Design and development of an underactuated prosthetic hand. In *Robotics and Automation, 2002. Proceedings. ICRA'02. IEEE International Conference on*, volume 4, pages 3374–3379. IEEE, 2002.

[9] C. Meijneke, G.A. Kragten, and M. Wisse. Design and performance assessment of an underactuated hand for industrial applications. 2011.

[10] F. Reuleaux. *Theoretische kinematik*. F. Vieweg und Sohn, 1875.

[11] Robotiq. Adaptive gripper, retrieved 23 november 2011 from http://robotiq.com.

[12] W. Townsend. The barretthand grasper–programmably flexible part handling and assembly. *Industrial Robot: an international journal*, 27(3):181–188, 2000.

APPENDIX A CE CONFIGURATIONS FOR CONSTRAINING AN OBJECT

In this appendix several CE configurations are presented that are able to completely restrain an object. The Figs A.1 - A.4 show a front view of the CE configurations in a plane. The CE can not make contact with the bottom the of the object since the objects are positioned on a flat surface.

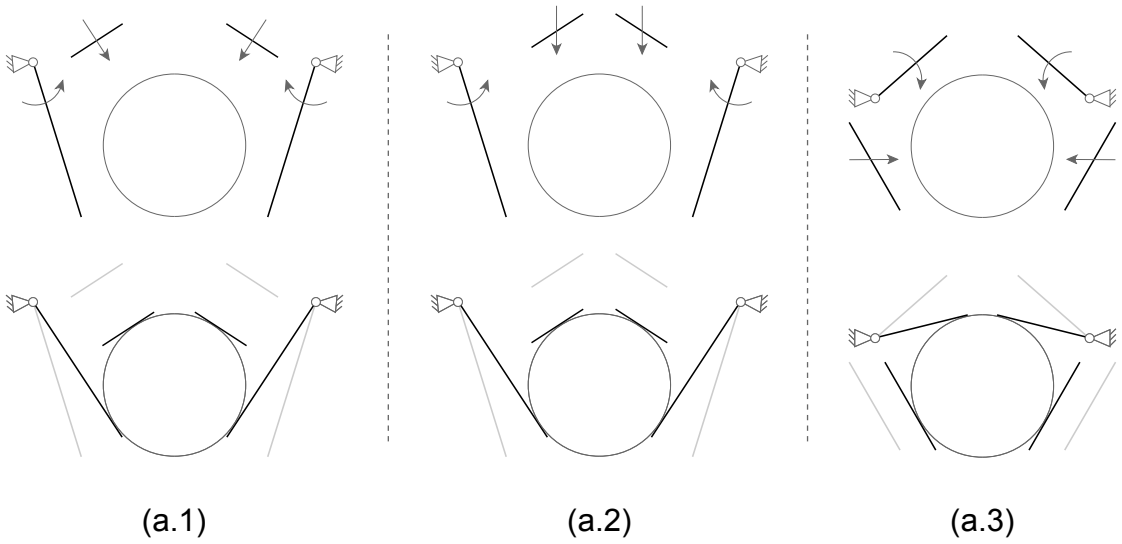

Figure A.1: Front view of three CE configurations in a plane. Each CE configuration has two rotating and two translating CE.

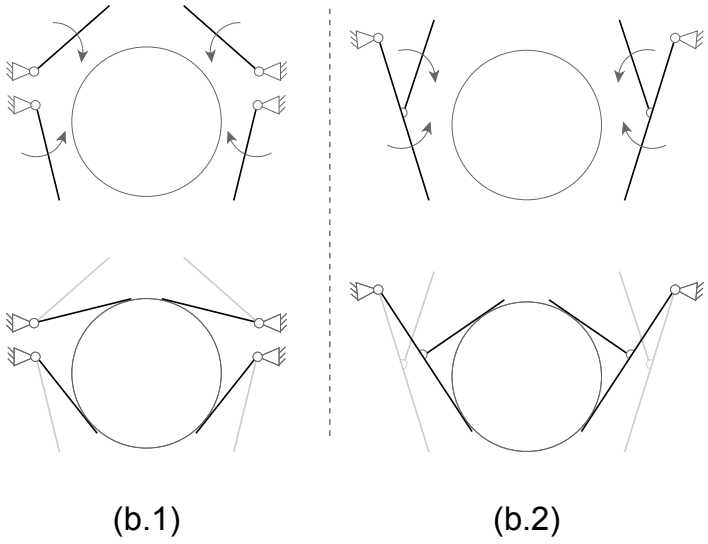

Figure A.2: Front view of two CE configurations in a plane. Both CE configuration have four rotating CE.

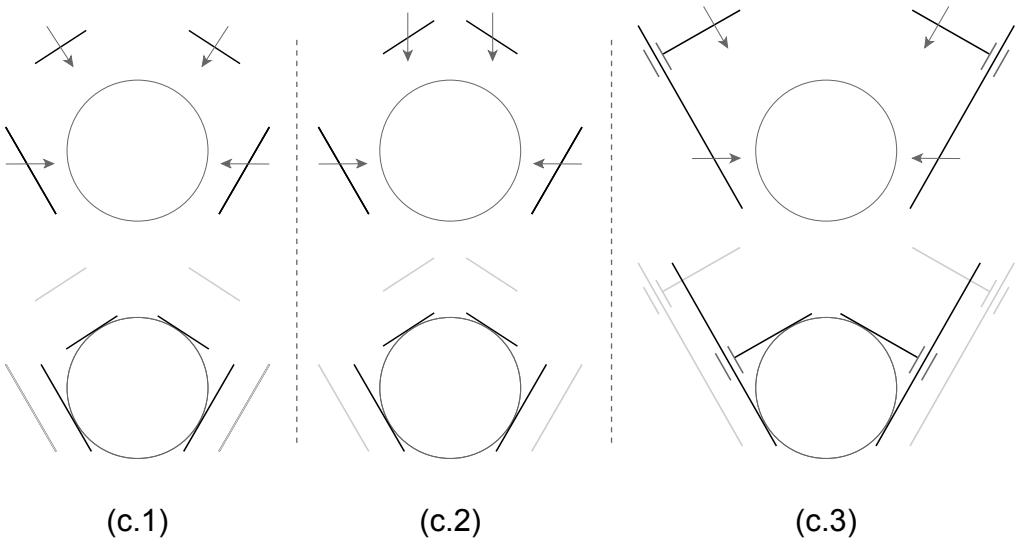

Figure A.3: Front view of three CE configurations in a plane. Each CE configuration has four translating CE.

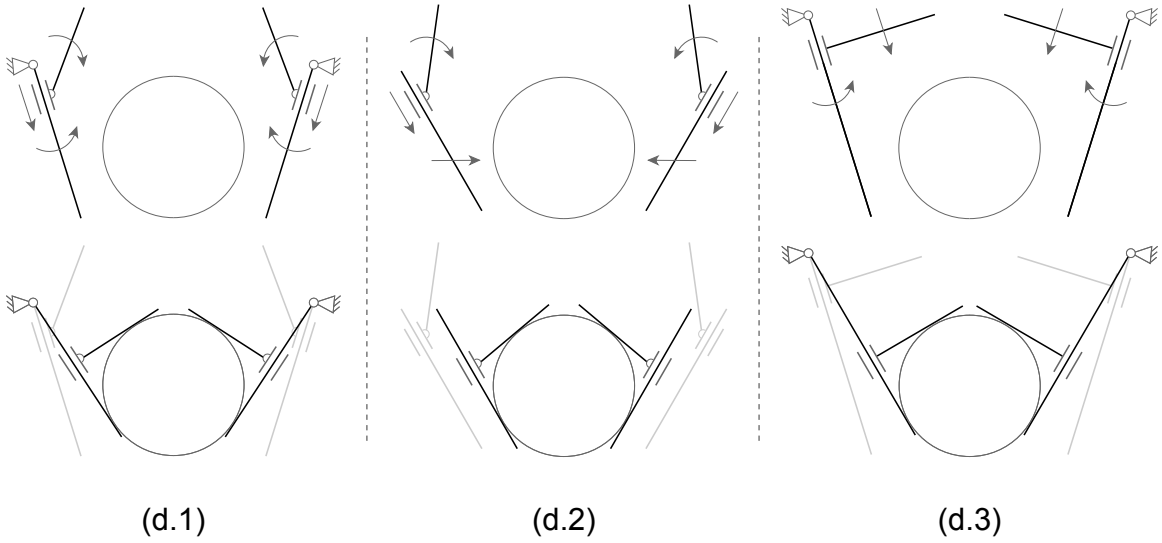

Figure A.4: Front view of three CE configurations in a plane. Each CE configuration has four CE of which two have a rotating and translating motion.

APPENDIX B DERIVING AN EXPRESSION FOR θ_1 AND θ_2 FROM THE CLOSED LOOP EQUATIONS

In this appendix the derivation of θ_1 and θ_2 from the loop closure vector equations is shown. The derivation can be used for the left side as well as the right side of the gripper. For the left side $\pm X_{obj} = -X_{obj}$, for the right side $\pm X_{obj} = X_{obj}$.

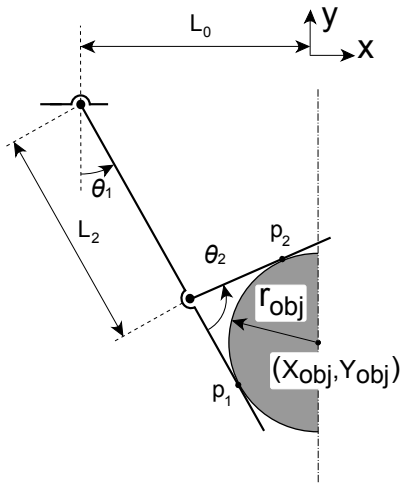

Figure B.1: Schematic of gripper with parameters for derivation of loop closure vector equation.

From Fig. B.1 the following loop closure vector equation can be derived for contact of the lower connecting element with the object,

$$\begin{pmatrix} -L_0 \\ 0 \end{pmatrix} + R_{\theta_1} \begin{pmatrix} 0 \\ -p_1 \end{pmatrix} = \begin{pmatrix} \pm X_{obj} \\ Y_{obj} \end{pmatrix} + R_{\theta_1} \begin{pmatrix} -r_{obj} \\ 0 \end{pmatrix} \tag{B.1}$$

From Eq. B.1 an expression for the contact point (p_1) on the lower connecting element can be obtained,

$$p_1 = \frac{Y_{obj} - r_{obj} \sin\theta_1}{-\cos\theta_1} \tag{B.2}$$

Now Eq. B.1 can be rearranged and when Eq. B.2 is used as an expression for p_1, Eq. B.1 can be written in the following form,

$$(\pm X_{obj} + L_0)\cos\theta_1 + Y_{obj}\sin\theta_1 = r_{obj} \tag{B.3}$$

The following general rule can be applied to Eq. B.3,

$$A\cos\theta + B\sin\theta = R\cos(\theta - \alpha)$$

where,

$$R = \sqrt{A^2 + B^2} \quad \text{and} \quad \alpha = \arctan\left(\tfrac{B}{A}\right)$$

From this, the following expression for θ_1 can be obtained,

$$\theta_1 = \arccos\left(\frac{r_{obj}}{\sqrt{(\pm X_{obj} + L_0)^2 + Y_{obj}^2}}\right) + \arctan\left(\frac{Y_{obj}}{\pm X_{obj} + L_0}\right) \tag{B.4}$$

From Fig. B.1 the following loop closure vector equation can be derived for contact of the upper connecting element with the object:

$$\begin{pmatrix} -L_0 \\ 0 \end{pmatrix} + R_{\theta_1} \begin{pmatrix} 0 \\ -L_2 \end{pmatrix} + R_{\theta_1} R_{\theta_2} \begin{pmatrix} 0 \\ -p_2 \end{pmatrix} = \begin{pmatrix} \pm X_{obj} \\ Y_{obj} \end{pmatrix} + R_{\theta_1} R_{\theta_2} \begin{pmatrix} r_{obj} \\ 0 \end{pmatrix} \tag{B.5}$$

From Eq. B.5 an expression for the contact point (p_2) on the upper connecting element can be obtained,

$$p_2 = \frac{Y_{obj} + L_2\cos\theta_1 + r_{obj}\sin(\theta_1 + \theta_2)}{-\cos(\theta_1 + \theta_2)} \tag{B.6}$$

Now Eq. B.5 can be rearranged and when Eq. B.6 is used as an expression for p_2, Eq. B.5 can be written in the following form,

$$(\pm X_{obj} + L_0 - L_2\sin\theta_1)\cos(\theta_1 + \theta_2) + (Y_{obj} + L_2\cos\theta_1)\sin(\theta_1 + \theta_2) = -r_{obj} \tag{B.7}$$

Using the standard form transformation, this gives the following expression for θ_2,

$$\theta_2 = \arccos\left(\frac{-r_{obj}}{\sqrt{(\pm X_{obj} + L_0 - L_2\sin\theta_1)^2 + (Y_{obj} + L_2\cos\theta_1)^2}}\right) + \arctan\left(\frac{Y_{obj} + L_2\cos\theta_1}{\pm X_{obj} + L_0 - L_2\sin\theta_1}\right) - \theta_1 \tag{B.8}$$

APPENDIX C DERIVING AN EXPRESSION FOR ANGLES ϕ_1 AND ϕ_2 TO DETERMINE THE CONFIGURATION OF THE ACTUATION MECHANISM

In this appendix the angles ϕ_1 and ϕ_2 are derived by means of trigonometry. The angles ϕ_1 and ϕ_2 describe the configuration of the actuation mechanism. The following trigonometric law is used,

Law of cosines: $c^2 = a^2 + b^2 - 2ab\cos\gamma$

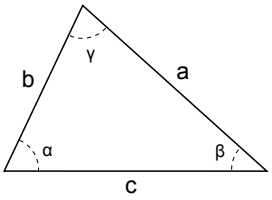

Figure C.1: Triangle with angles and sides labeled for law of cosines.

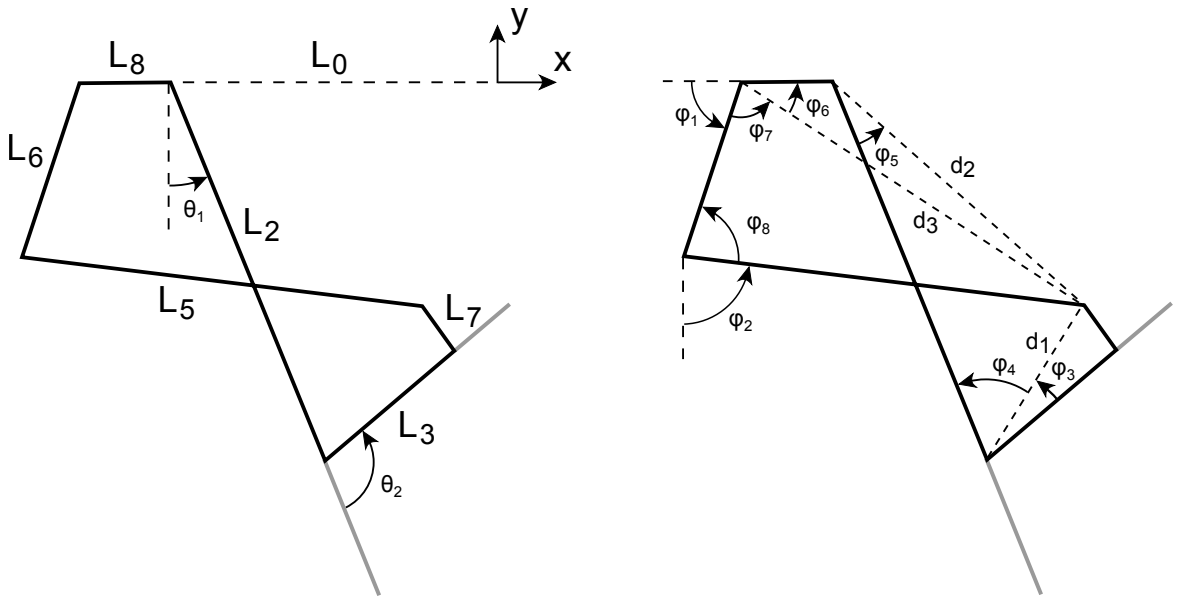

Figure C.2: A labelled representation of the gripper segments and important angles.

Figure C.2 shows the angles and parameters of the system. To derive an expression for ϕ_1 and ϕ_2, first distance d_1 and angle ϕ_3 are calculated,

$$d_1 = \sqrt{{L_3}^2 + {L_7}^2} \tag{C.1}$$

$$\phi_3 = \arccos\frac{L_3}{d_1} \tag{C.2}$$

Angle θ_2 and ϕ_3 are used to obtain an expression for ϕ_4,

$$\phi_4 = \pi - \theta_2 - \phi_3 \tag{C.3}$$

Using the law of cosines in combination with d_1 and ϕ_4 gives the following expression for d_2,

$$d_2 = \sqrt{{L_2}^2 + {d_1}^2 - 2L_2 d_1\cos\phi_4} \tag{C.4}$$

Using the law of cosines in combination with d_1, d_2 and ϕ_4, an expression for ϕ_5 is obtained,

$$\phi_5 = \begin{cases} \arccos\left(\frac{{d_1}^2 - {L_2}^2 - {d_2}^2}{-2L_2 d_2}\right) & : \phi_4 \geq 0 \\ -\arccos\left(\frac{{d_1}^2 - {L_2}^2 - {d_2}^2}{-2L_2 d_2}\right) & : \phi_4 < 0 \end{cases} \tag{C.5}$$

Using ϕ_5 and θ_1, distance d_3 can be determined with help of the law of cosines,

$$d_3 = \sqrt{{d_2}^2 + {L_8}^2 - 2d_2 L_8\cos\left(\frac{\pi}{2} + \theta_1 + \phi_5\right)} \tag{C.6}$$

With d_2 and d_3 known, an expression for ϕ_6, ϕ_7 and ϕ_8 can be obtained. Angles ϕ_6, ϕ_7 and ϕ_8 are obtained by applying the law of cosines,

$$\phi_6 = \begin{cases} \arccos\left(\frac{{d_2}^2-{L_8}^2-{d_3}^2}{-2L_8 d_3}\right) & : \theta_1 + \phi_5 \leq \frac{\pi}{2} \\ -\arccos\left(\frac{{d_2}^2-{L_8}^2-{d_3}^2}{-2L_8 d_3}\right) & : \theta_1 + \phi_5 > \frac{\pi}{2} \end{cases} \tag{C.7}$$

$$\phi_7 = \arccos\left(\frac{{L_5}^2 - {d_3}^2 - {L_6}^2}{-2d_3 L_6}\right) \tag{C.8}$$

$$\phi_8 = \arccos\left(\frac{{d_3}^2 - {L_5}^2 - {L_6}^2}{-2L_5 L_6}\right) \tag{C.9}$$

Finally, an expression for ϕ_1 and ϕ_2 can be obtained,

$$\phi_1 = \pi - \phi_6 - \phi_7 = \begin{cases} \pi - \arccos\left(\frac{{d_2}^2-{L_8}^2-{d_3}^2}{-2L_8 d_3}\right) - \arccos\left(\frac{{L_5}^2-{d_3}^2-{L_6}^2}{-2d_3 L_6}\right) & : \theta_1 + \phi_5 \leq \frac{\pi}{2} \\ \pi + \arccos\left(\frac{{d_2}^2-{L_8}^2-{d_3}^2}{-2L_8 d_3}\right) - \arccos\left(\frac{{L_5}^2-{d_3}^2-{L_6}^2}{-2d_3 L_6}\right) & : \theta_1 + \phi_5 > \frac{\pi}{2} \end{cases} \tag{C.10}$$

$$\phi_2 = \frac{\pi}{2} + \phi_1 - \phi_8 = \frac{\pi}{2} + \phi_1 - \arccos\left(\frac{{d_3}^2 - {L_5}^2 - {L_6}^2}{-2L_5 L_6}\right) \tag{C.11}$$

APPENDIX D DETERMINE FORCES IN FRICTIONLESS SYSTEM BY MEANS OF A FREE BODY DIAGRAM

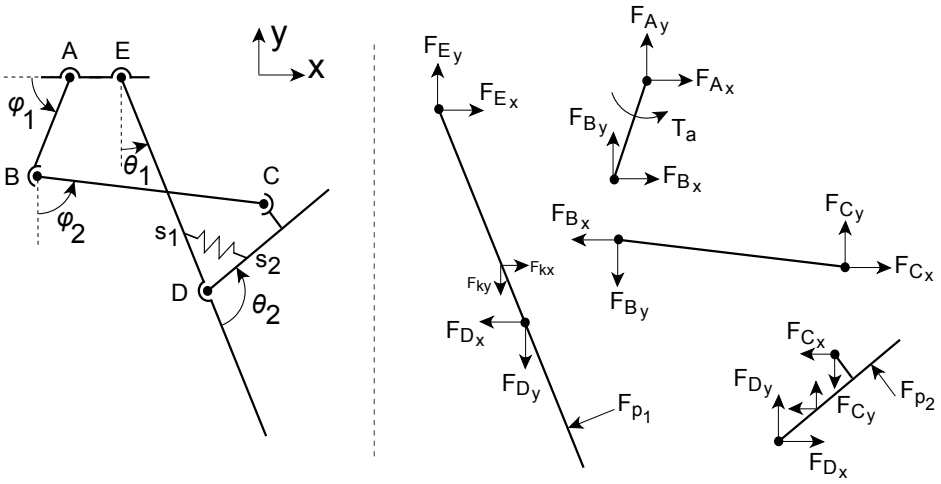

Figure D.1: Free body diagram of the gripper.

Linkage AB

$$F_{A_x} + F_{B_x} = 0 \tag{D.1}$$

$$F_{A_y} + F_{B_y} = 0 \tag{D.2}$$

$$F_{B_x} L_6 \sin\phi_1 - F_{B_y} L_6 \cos\phi_1 = -T_a \tag{D.3}$$

Linkage BC

$$F_{C_x} - F_{B_x} = 0 \tag{D.4}$$

$$F_{C_y} - F_{B_y} = 0 \tag{D.5}$$

$$F_{C_x} L_5 \cos\phi_2 + F_{C_y} L_5 \sin\phi_2 = 0 \tag{D.6}$$

Linkage CD

$$F_{D_x} - F_{C_x} + F_{p2}\cos(\theta_1 + \theta_2) = F_{k_x} \tag{D.7}$$

$$F_{D_y} - F_{C_y} + F_{p2}\sin(\theta_1 + \theta_2) = -F_{k_y} \tag{D.8}$$

$$\begin{aligned} F_{C_x}\left(L_7\sin(\theta_1+\theta_2) - L_3\cos(\theta_1+\theta_2)\right) - F_{C_y}\left(L_7\cos(\theta_1+\theta_2) + L_3\sin(\theta_1+\theta_2)\right)\ldots \\ + p_2 F_{p2} = F_{k_x} s_1 \cos(\theta_1+\theta_2) - F_{k_y} s_1 \sin(\theta_1+\theta_2) \end{aligned} \tag{D.9}$$

Linkage DE

$$F_{E_x} - F_{D_x} - F_{p1}\cos\theta_1 = -F_{k_x} \tag{D.10}$$

$$F_{E_y} - F_{D_y} - F_{p1}\sin\theta_1 = F_{k_y} \tag{D.11}$$

$$-F_{D_x} L_2 \cos\theta_1 - F_{D_y} L_2 \sin\theta_1 - p_1 F_{p1} = F_{k_y}(L_2 - s_2)\sin\theta_1 - F_{k_x}(L_2 - s_2)\cos\theta_1 \tag{D.12}$$

To derive the horizontal and vertical components of the spring force, first the spring force F_k needs to be determined,

$$F_k = k\left(L_k - L_{k0}\right) \tag{D.13}$$

where, k is the spring constant, L_{k0} is the initial spring length and L_k the current spring length, which is calculated as follows,

$$L_k = \sqrt{{s_1}^2 + {s_2}^2 - 2 s_1 s_2 \cos(\pi - \theta_2)} \tag{D.14}$$

The horizontal and vertical components of the spring forces (F_{k_x} and F_{k_y}) are calculated as follows,

$$F_{k_x} = F_k \sin(\theta_1 + \alpha) \tag{D.15}$$

$$F_{k_y} = F_k \cos(\theta_1 + \alpha) \tag{D.16}$$

with,

$$\alpha = \arccos\left(\frac{{s_1}^2 - {s_2}^2 - {L_k}^2}{-2 s_2 L_k}\right) \tag{D.17}$$

APPENDIX E GRAPHICAL USER INTERFACE FOR FRICTIONLESS MODEL

In this appendix the graphical user interface (GUI) that is used to explore the frictionless gripper model is described. An overview of the GUI is given and the MATLAB code of the most important function is given.

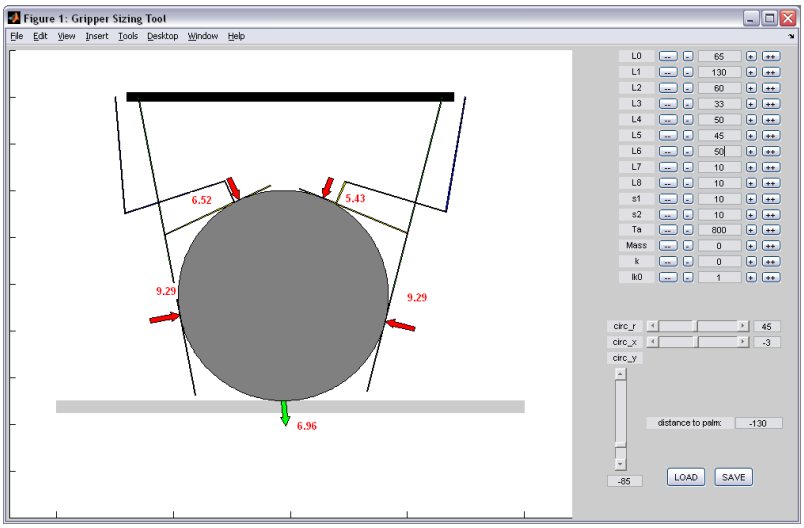

Figure E.1: Graphical user interface for examining gripper mechanism.

Figure E.1 shows the GUI. The following parameters can be adjusted:

- The design parameters (L_0, L_1, L_2, L_3, L_4, L_5, L_6, L_7, L_8, s_1, s_2), where s_1 and s_2 are the distance between the spring connection point on the UCE and LCE, respectively, and joint D.
- The actuation torque (T_a).
- Object properties ($Mass$, $circ_r$, $circ_x$ and $circ_y$), where $circ_r$, $circ_x$ and $circ_y$ are the radius, horizontal position with respect to gripper and vertical position with respect to the gripper, respectively.
- Spring properties (k, $lk0$), where k is the spring constant and $lk0$ is the initial spring lenght.

In the GUI the contact positions and magnitude of the forces applied by the CE onto the object are shown. The contact forces shown, are calculated under the assumption that the object is fixed. Therefore, force equilibrium of gripper and object can only exist when the applied forces by the CE and all other forces active on the object equilibrate each other. The resulting force on the object, if present, is presented by the green arrow at the bottom of the object. The green arrow indicates the magnitude as well as the direction of the resulting force.

In Fig. E.2 the MATLAB code is shown that is used to calculate the contact forces between object and gripper that are needed to achieve force equilibrium of the gripper.

```
%%%%%%%%%%%%%%%%%%%%%%%%%%%%%%%%%%%%%%%%%%%%%%%%%%%%%%%%%%%%%%%%%%%%%%%%%%%%%%%%
%%%                                                                           %%%
%%% Function that calculates the forces applied by the CE onto the object.   %%%
%%%                                                                           %%%
%%% Input "Param" comprises - the design parameters: L2, L3, L5, L6 and L7    %%%
%%%                         - distance spring connections - joint D: s1 and s2 %%%
%%%                         - spring constant and initial length: k and lk0   %%%
%%%                         - the actuation torque: Ta                        %%%
%%% Input "Angles" comprises the angles: theta1, theta2, phi1 and phi2.       %%%
%%% Input "ContP" comprises the contact points: p1 and p2.                    %%%
%%%                                                                           %%%
%%%%%%%%%%%%%%%%%%%%%%%%%%%%%%%%%%%%%%%%%%%%%%%%%%%%%%%%%%%%%%%%%%%%%%%%%%%%%%%%
function Fn = Forces(Param,Angles,ContP)

% Calculate spring force components
lk = sqrt(s1^2 + s2^2 - 2*s1*s2*cos(pi - th2));   % length active spring
Fk = k*(lk - lk0);                                % spring force
alpha = acos((s1^2 - s2^2 - lk^2)/(-2*s2*lk));    % orientation spring with respect to LCE
Fkx = Fk*sin(th1 + alpha);                        % horizontal spring force component
Fky = Fk*cos(th1 + alpha);                        % vertical spring force component

% Force equilibrium components
S3_3 = L6*sin(phi1);                              S3_4 = -L6*cos(phi1);
S6_5 = L5*cos(phi2);                              S6_6 = L5*sin(phi2);
S7_12 = cos(th1 + th2);                           S8_12 = sin(th1 + th2);
S9_5 = (L7*sin(th1 + th2)-L3*cos(th1 + th2));     S9_6 = -(L3*sin(th1 + th2) + L7*cos(th1 + th2));
S10_11 = -cos(th1);
S11_11 = -sin(th1);
S12_7 = -L2*cos(th1);                             S12_8 = -L2*sin(th1);

% matrix with equilibrium equation
%   F_Ax    F_Ay    F_Bx    F_By    F_Cx    F_Cy    F_Dx    F_Dy    F_Ex    F_Ey    F_p1    F_p2
S = [ 1     0       1       0       0       0       0       0       0       0       0       0
      0     1       0       1       0       0       0       0       0       0       0       0
      0     0       S3_3    S3_4    0       0       0       0       0       0       0       0
      0     0       -1      0       1       0       0       0       0       0       0       0
      0     0       0       -1      0       1       0       0       0       0       0       0
      0     0       0       0       S6_5    S6_6    0       0       0       0       0       0
      0     0       0       0       -1      0       1       0       0       0       0       S7_12
      0     0       0       0       0       -1      0       1       0       0       0       S8_12
      0     0       0       0       S9_5    S9_6    0       0       0       0       0       p2
      0     0       0       0       0       0       -1      0       1       0       S10_11  0
      0     0       0       0       0       0       0       -1      0       1       S11_11  0
      0     0       0       0       0       0       S12_7   S12_8   0       0       -p1     0];

% Vector with external forces
F = [0 0 -Ta 0 0 0 Fkx -Fky (Fkx*s1*cos(th1 + th2) - ...
    Fky*s1*(sin(th1 + th2))) -Fkx Fky (Fky*(L2 - s2)*sin(th1) - ...
    Fkx*(L2 - s2)*cos(th1))]';

X = S\F;                % calculate reaction forces in system

Fn = [X(11); X(12)];    % vector with forces applied onto the object, Fn = [F_p1; F_p2]
end
```

Figure E.2: MATLAB code - function that returns the contact forces required for force equilibrium of gripper.

APPENDIX F DETERMINE FORCES IN SYSTEM BY MEANS OF A FREE BODY DIAGRAM

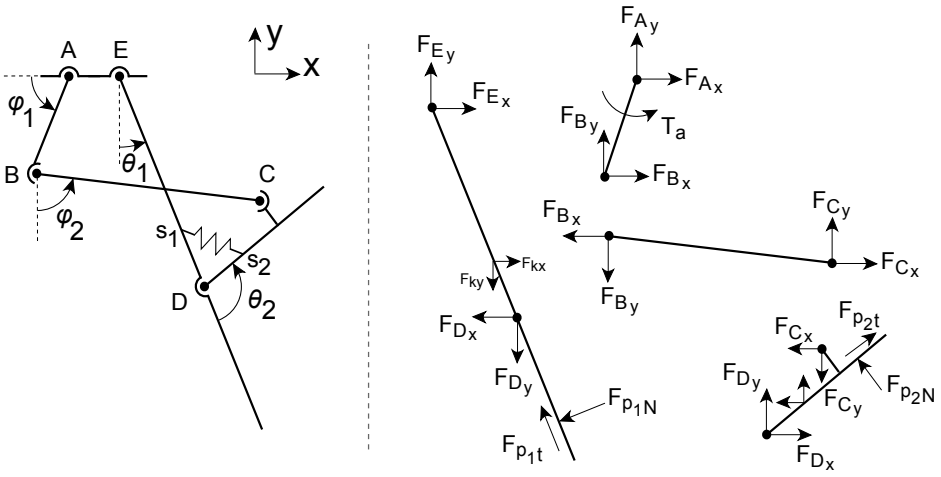

Figure F.1: Free body diagram of the gripper.

Linkage AB

$$F_{A_x} + F_{B_x} = 0 \tag{F.1}$$

$$F_{A_y} + F_{B_y} = 0 \tag{F.2}$$

$$F_{B_x} L_6 \sin\phi_1 - F_{B_y} L_6 \cos\phi_1 = -T_a \tag{F.3}$$

Linkage BC

$$F_{C_x} - F_{B_x} = 0 \tag{F.4}$$

$$F_{C_y} - F_{B_y} = 0 \tag{F.5}$$

$$F_{C_x} L_5 \cos\phi_2 + F_{C_y} L_5 \sin\phi_2 = 0 \tag{F.6}$$

Linkage CD

$$F_{D_x} - F_{C_x} + F_{p2_N} \cos(\theta_1 + \theta_2) + F_{p2_t} \sin(\theta_1 + \theta_2) = F_{k_x} \tag{F.7}$$

$$F_{D_y} - F_{C_y} + F_{p2_N} \sin(\theta_1 + \theta_2) - F_{p2_t} \cos(\theta_1 + \theta_2) = -F_{k_y} \tag{F.8}$$

$$\begin{aligned} F_{C_x}(L_7 \sin(\theta_1 + \theta_2) - L_3 \cos(\theta_1 + \theta_2)) - F_{C_y}(L_7 \cos(\theta_1 + \theta_2) + L_3 \sin(\theta_1 + \theta_2)) \ldots \\ + p_2 F_{p2_N} = F_{k_x} s_1 \cos(\theta_1 + \theta_2) - F_{k_y} s_1 \sin(\theta_1 + \theta_2) \end{aligned} \tag{F.9}$$

Linkage DE

$$F_{E_x} - F_{D_x} - F_{p1_N} \cos\theta_1 - F_{p1_t} \sin\theta_1 = -F_{k_x} \tag{F.10}$$

$$F_{E_y} - F_{D_y} - F_{p1_N} \sin\theta_1 + F_{p1_t} \cos\theta_1 = F_{k_y} \tag{F.11}$$

$$-F_{D_x} L_2 \cos\theta_1 - F_{D_y} L_2 \sin\theta_1 - p_1 F_{p1_N} = F_{k_y}(L_2 - s_2)\sin\theta_1 - F_{k_x}(L_2 - s_2)\cos\theta_1 \tag{F.12}$$

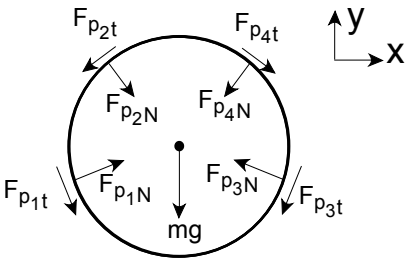

Figure F.2: Free body diagram of the object.

Object

$$F_{p1_x} + F_{p2_x} + F_{p3_x} + F_{p4_x} = 0 \tag{F.13}$$

$$F_{p1_y} + F_{p2_y} + F_{p3_y} + F_{p4_y} - mg = 0 \tag{F.14}$$

$$(F_{p1_t} + F_{p2_t} - F_{p3_t} - F_{p4_t})\, r_{obj} = 0 \tag{F.15}$$

where,

$$\begin{pmatrix} F_{p1_x} \\ F_{p1_y} \end{pmatrix} = R_{\theta_1} \begin{pmatrix} F_{p1_N} \\ 0 \end{pmatrix} + R_{\theta_1} \begin{pmatrix} 0 \\ -F_{p1_t} \end{pmatrix} = \begin{pmatrix} F_{p1_N}\cos\theta_1 + F_{p1_t}\sin\theta_1 \\ F_{p1_N}\sin\theta_1 - F_{p1_t}\cos\theta_1 \end{pmatrix} \tag{F.16}$$

$$\begin{pmatrix} F_{p2_x} \\ F_{p2_y} \end{pmatrix} = R_{\theta_1} R_{\theta_2} \begin{pmatrix} -F_{p2_N} \\ 0 \end{pmatrix} + R_{\theta_1} R_{\theta_2} \begin{pmatrix} 0 \\ F_{p2_t} \end{pmatrix} = \begin{pmatrix} -F_{p2_N} \cos(\theta_1 + \theta_2) - F_{p2_t} \sin(\theta_1 + \theta_2) \\ -F_{p2_N} \sin(\theta_1 + \theta_2) + F_{p2_t} \cos(\theta_1 + \theta_2) \end{pmatrix} \tag{F.17}$$

$$\begin{pmatrix} F_{p3_x} \\ F_{p3_y} \end{pmatrix} = R_{(-\theta_1)} \begin{pmatrix} -F_{p3_N} \\ 0 \end{pmatrix} + R_{(-\theta_3)} \begin{pmatrix} 0 \\ -F_{p3_t} \end{pmatrix} = \begin{pmatrix} -F_{p3_N} \cos(-\theta_3) + F_{p3_t} \sin(-\theta_3) \\ -F_{p3_N} \sin(-\theta_3) - F_{p3_t} \cos(-\theta_3) \end{pmatrix} \tag{F.18}$$

$$\begin{pmatrix} F_{p4_x} \\ F_{p4_y} \end{pmatrix} = R_{(-\theta_3)} R_{(-\theta_4)} \begin{pmatrix} F_{p4_N} \\ 0 \end{pmatrix} + R_{(-\theta_3)} R_{(-\theta_4)} \begin{pmatrix} 0 \\ F_{p4_t} \end{pmatrix} = \begin{pmatrix} F_{p4_N} \cos(-\theta_3 - \theta_4) - F_{p4_t} \sin(-\theta_3 - \theta_4) \\ F_{p4_N} \sin(-\theta_3 - \theta_4) + F_{p4_t} \cos(-\theta_3 - \theta_4) \end{pmatrix} \tag{F.19}$$

with,

$$R_\theta = \begin{pmatrix} \cos\theta & -\sin\theta \\ \sin\theta & \cos\theta \end{pmatrix} \tag{F.20}$$

To derive the horizontal and vertical components of the spring force, first the spring force F_k needs to be determined,

$$F_k = k(L_k - L_{k0}) \tag{F.21}$$

where, k is the spring constant, L_{k0} is the initial spring length and L_k the current spring length, which is calculated as follows,

$$L_k = \sqrt{{s_1}^2 + {s_2}^2 - 2 s_1 s_2 \cos(\pi - \theta_2)} \tag{F.22}$$

The horizontal and vertical components of the spring forces (F_{k_x} and F_{k_y}) are calculated as follows,

$$F_{k_x} = F_k \sin(\theta_1 + \alpha) \tag{F.23}$$

$$F_{k_y} = F_k \cos(\theta_1 + \alpha) \tag{F.24}$$

with,

$$\alpha = \arccos\left(\frac{{s_1}^2 - {s_2}^2 - {L_k}^2}{-2 s_2 L_k}\right) \tag{F.25}$$

APPENDIX G MINIMUM REQUIRED COEFFICIENT OF FRICTION - RESULTS OPTIMISATION PROCESS

Table G.1: Results from the optimisation process for massless circular objects ranging from 60mm to 120mm diameter and a horizontal displacement of ±6mm. The starting value sets can be found in Table 4. The fixed design parameters used in the optimisation process were L_0, L_1 and L_2. A Q-value of 1.00 represents a complete feasible grasp range for the presented design parameters and coefficient of friction (μ).

Starting value set	μ	Q	L_0 [mm]	L_1 [mm]	L_2 [mm]	L_3 [mm]	L_5 [mm]	L_6 [mm]	L_7 [mm]	L_8 [mm]
1	0.40	1.00	103.5	200.0	50.0	10.0	35.0	30.0	20.0	10.0
2	0.40	1.00	103.5	200.0	50.0	10.0	50.0	45.0	25.0	20.0
3	0.40	1.00	103.5	200.0	50.0	20.0	70.0	20.0	15.0	10.0
4	0.40	1.00	103.5	200.0	50.0	20.0	50.0	40.0	25.0	25.0
5	0.40	1.00	103.5	200.0	50.0	30.0	50.0	40.0	25.0	10.0
6	0.40	1.00	103.5	200.0	50.0	30.0	70.0	25.0	15.0	20.0
7	0.40	1.00	103.5	200.0	50.0	40.0	80.0	20.0	15.0	15.0
8	0.40	1.00	103.5	200.0	50.0	40.0	90.0	30.0	30.0	25.0
9	0.40	1.00	103.5	200.0	50.0	50.0	90.0	25.0	30.0	10.0
10	0.40	1.00	103.5	200.0	50.0	50.0	100.0	15.0	15.0	20.0
11	0.40	1.00	103.5	200.0	50.0	60.0	90.0	25.0	10.0	5.0
12	0.40	1.00	103.5	200.0	50.0	60.0	110.0	15.0	25.0	20.0
13	0.40	1.00	103.5	200.0	50.0	70.0	100.0	30.0	25.0	10.0
14	0.40	1.00	103.5	200.0	50.0	70.0	120.0	15.0	30.0	15.0
15	0.40	1.00	103.5	200.0	50.0	80.0	110.0	35.0	30.0	15.0
16	0.40	1.00	103.5	200.0	50.0	80.0	130.0	25.0	40.0	25.0
1	0.30	1.00	103.5	200.0	50.0	10.0	35.0	30.0	20.0	10.0
2	0.30	1.00	103.5	200.0	50.0	10.0	50.0	45.0	25.0	20.0
3	0.30	1.00	103.5	200.0	50.0	20.0	70.0	20.0	15.0	10.0
4	0.30	1.00	103.5	200.0	50.0	20.0	50.0	40.0	25.0	25.0
5	0.30	1.00	103.5	200.0	50.0	30.0	50.0	40.0	25.0	10.0
6	0.30	1.00	103.5	200.0	50.0	30.0	70.0	25.0	15.0	20.0
7	0.30	1.00	103.5	200.0	50.0	40.0	80.0	20.0	15.0	15.0
8	0.30	1.00	103.5	200.0	50.0	40.0	90.0	30.0	30.0	25.0
9	0.30	1.00	103.5	200.0	50.0	50.0	90.0	25.0	30.0	10.0
10	0.30	1.00	103.5	200.0	50.0	50.0	100.0	15.0	15.0	20.0
11	0.30	1.00	103.5	200.0	50.0	60.0	90.0	25.0	10.0	5.0
12	0.30	1.00	103.5	200.0	50.0	61.1	109.4	15.6	22.8	20.8
13	0.30	1.00	103.5	200.0	50.0	70.0	100.0	30.0	25.0	10.0
14	0.30	1.00	103.5	200.0	50.0	72.6	113.5	17.4	23.4	15.2
15	0.30	1.00	103.5	200.0	50.0	80.0	110.0	35.0	30.0	15.0
16	0.30	1.00	103.5	200.0	50.0	80.0	130.0	25.0	40.0	25.0
1	0.20	1.00	103.5	200.0	50.0	10.0	35.0	30.0	20.0	10.0
2	0.20	1.00	103.5	200.0	50.0	9.9	51.1	39.7	27.4	21.9
3	0.20	1.00	103.5	200.0	50.0	20.4	56.8	23.0	14.8	10.8
4	0.20	1.00	103.5	200.0	50.0	20.0	50.0	40.0	25.0	25.0
5	0.20	1.00	103.5	200.0	50.0	30.0	50.0	40.0	25.0	10.0
6	0.20	1.00	103.5	200.0	50.0	30.0	70.0	25.0	15.0	20.0
7	0.20	1.00	103.5	200.0	50.0	40.0	80.0	21.0	15.0	15.0
8	0.20	1.00	103.5	200.0	50.0	40.8	85.5	30.6	30.6	25.5
9	0.20	1.00	103.5	200.0	50.0	50.1	81.5	28.3	27.6	10.6
10	0.20	0.93	103.5	200.0	50.0	50.6	99.4	15.4	14.7	20.8
11	0.20	1.00	103.5	200.0	50.0	63.0	90.0	25.0	10.0	5.0
12	0.20	0.94	103.5	200.0	50.0	59.9	108.2	17.6	17.8	22.7
13	0.20	1.00	103.5	200.0	50.0	73.5	100.0	30.0	25.0	10.0
14	0.20	1.00	103.5	200.0	50.0	78.5	113.9	23.2	17.0	14.0
15	0.20	1.00	103.5	200.0	50.0	84.0	110.0	35.0	30.0	15.0
16	0.20	1.00	103.5	200.0	50.0	83.1	128.0	27.0	35.7	26.4
1	0.10	1.00	103.5	200.0	50.0	9.2	27.7	37.0	16.9	10.7
2	0.10	1.00	103.5	200.0	50.0	12.0	31.3	48.1	29.6	20.4
3	0.10	0.81	103.5	200.0	50.0	25.4	59.5	21.6	10.7	11.5

Continued on Next Page...

Table G.1 – Continued

Starting value set	μ	Q	L_0 [mm]	L_1 [mm]	L_2 [mm]	L_3 [mm]	L_5 [mm]	L_6 [mm]	L_7 [mm]	L_8 [mm]
4	0.10	1.00	103.5	200.0	50.0	21.0	49.2	40.8	25.8	24.0
5	0.10	1.00	103.5	200.0	50.0	31.0	48.1	38.4	25.8	10.3
6	0.10	0.83	103.5	200.0	50.0	31.3	60.7	30.7	15.1	18.6
7	0.10	0.72	103.5	200.0	50.0	40.7	79.0	20.3	15.5	14.7
8	0.10	1.00	103.5	200.0	50.0	43.8	72.7	40.1	34.1	22.7
9	0.10	1.00	103.5	200.0	50.0	54.6	71.7	38.9	29.4	9.2
10	0.10	0.74	103.5	200.0	50.0	43.7	74.2	27.6	11.8	17.4
11	0.10	0.86	103.5	200.0	50.0	63.3	89.2	25.9	9.9	4.9
12	0.10	0.58	103.5	200.0	50.0	60.0	110.0	15.8	25.0	20.0
13	0.10	1.00	103.5	200.0	50.0	71.9	94.7	33.3	25.2	10.1
14	0.10	0.63	103.5	200.0	50.0	78.2	118.6	18.6	19.0	16.2
15	0.10	1.00	103.5	200.0	50.0	83.9	109.3	34.4	31.2	15.0
16	0.10	1.00	103.5	200.0	50.0	64.1	92.5	40.2	40.9	21.4
1	0.09	1.00	103.5	200.0	50.0	10.3	29.5	36.5	14.8	11.6
2	0.09	1.00	103.5	200.0	50.0	10.5	29.7	47.8	25.0	22.8
3	0.09	0.95	103.5	200.0	50.0	19.0	43.9	30.9	13.1	12.1
4	0.09	1.00	103.5	200.0	50.0	25.0	48.6	40.6	27.9	17.5
5	0.09	1.00	103.5	200.0	50.0	31.0	48.1	38.4	25.8	10.3
6	0.09	0.80	103.5	200.0	50.0	31.5	59.1	32.0	15.2	18.2
7	0.09	0.65	103.5	200.0	50.0	42.0	80.0	20.0	15.0	15.0
8	0.09	0.81	103.5	200.0	50.0	39.8	72.6	35.2	25.8	26.2
9	0.09	1.00	103.5	200.0	50.0	54.4	73.8	36.4	26.8	10.4
10	0.09	0.50	103.5	200.0	50.0	51.2	98.0	15.0	15.3	20.2
11	0.09	1.00	103.5	200.0	50.0	64.8	83.7	31.9	8.8	4.9
12	0.09	0.54	103.5	200.0	50.0	59.2	110.2	15.2	25.4	20.3
13	0.09	1.00	103.5	200.0	50.0	81.4	100.9	34.3	22.9	9.1
14	0.09	1.00	103.5	200.0	50.0	86.8	107.5	29.3	−0.4	3.3
15	0.09	0.99	103.5	200.0	50.0	83.6	107.5	35.1	30.4	14.5
16	0.09	0.66	103.5	200.0	50.0	82.6	126.9	26.0	40.1	24.9
1	0.08	1.00	103.5	200.0	50.0	11.0	27.9	37.7	17.1	10.5
2	0.08	1.00	103.5	200.0	50.0	11.5	33.8	44.4	25.2	21.0
3	0.08	0.81	103.5	200.0	50.0	26.8	53.9	27.0	10.1	10.7
4	0.08	1.00	103.5	200.0	50.0	27.0	46.2	41.1	32.6	12.0
5	0.08	1.00	103.5	200.0	50.0	31.0	48.1	38.4	25.8	10.3
6	0.08	0.73	103.5	200.0	50.0	31.8	58.5	32.8	14.6	18.9
7	0.08	0.63	103.5	200.0	50.0	41.4	78.3	21.1	15.0	14.8
8	0.08	1.00	103.5	200.0	50.0	38.1	63.9	41.9	34.4	21.0
9	0.08	1.00	103.5	200.0	50.0	50.4	63.8	41.2	27.1	9.5
10	0.08	0.45	103.5	200.0	50.0	51.1	97.4	15.6	15.0	20.2
11	0.08	1.00	103.5	200.0	50.0	60.3	77.5	33.2	9.9	5.1
12	0.08	0.50	103.5	200.0	50.0	59.8	108.8	15.6	25.9	19.9
13	0.08	0.86	103.5	200.0	50.0	72.1	98.0	30.5	25.5	10.2
14	0.08	0.50	103.5	200.0	50.0	73.0	119.0	15.8	24.9	16.7
15	0.08	0.94	103.5	200.0	50.0	83.1	107.6	34.6	30.7	14.5
16	0.08	0.96	103.5	200.0	50.0	59.1	84.7	41.7	37.1	22.1
1	0.07	1.00	103.5	200.0	50.0	11.1	28.3	37.8	16.7	10.4
2	0.07	1.00	103.5	200.0	50.0	10.9	29.3	48.3	27.1	21.9
3	0.07	0.99	103.5	200.0	50.0	26.8	44.1	34.0	11.6	6.5
4	0.07	1.00	103.5	200.0	50.0	24.0	42.6	45.1	29.7	18.3
5	0.07	1.00	103.5	200.0	50.0	31.1	47.7	39.1	25.9	10.3
6	0.07	1.00	103.5	200.0	50.0	17.8	36.0	39.1	20.9	12.2
7	0.07	0.55	103.5	200.0	50.0	41.4	79.0	20.4	15.0	15.1
8	0.07	0.65	103.5	200.0	50.0	41.9	81.7	30.2	31.4	25.3
9	0.07	1.00	103.5	200.0	50.0	44.1	60.4	39.2	29.7	9.7
10	0.07	0.40	103.5	200.0	50.0	51.8	98.5	14.8	15.4	20.3

Continued on Next Page...

Table G.1 – Continued

Starting value set	μ	Q	L_0 [mm]	L_1 [mm]	L_2 [mm]	L_3 [mm]	L_5 [mm]	L_6 [mm]	L_7 [mm]	L_8 [mm]
11	0.07	0.73	103.5	200.0	50.0	62.0	88.3	25.3	10.2	5.0
12	0.07	0.44	103.5	200.0	50.0	59.0	109.3	15.1	25.9	20.7
13	0.07	0.99	103.5	200.0	50.0	69.6	89.0	35.7	24.2	10.5
14	0.07	0.46	103.5	200.0	50.0	72.2	116.3	16.4	22.9	16.8
15	0.07	0.94	103.5	200.0	50.0	82.9	104.7	37.1	30.9	15.0
16	0.07	0.54	103.5	200.0	50.0	81.4	127.1	25.2	40.9	25.4
1	0.06	0.98	103.5	200.0	50.0	9.9	25.0	40.2	18.5	10.9
2	0.06	1.00	103.5	200.0	50.0	10.8	30.1	46.7	28.8	20.5
3	0.06	0.79	103.5	200.0	50.0	16.4	38.6	31.1	10.3	10.1
4	0.06	0.93	103.5	200.0	50.0	23.0	43.6	45.8	28.2	23.0
5	0.06	0.98	103.5	200.0	50.0	31.0	47.1	39.8	26.2	10.4
6	0.06	0.99	103.5	200.0	50.0	22.7	40.5	41.0	26.1	13.3
7	0.06	0.49	103.5	200.0	50.0	40.6	78.0	20.3	15.2	15.2
8	0.06	0.58	103.5	200.0	50.0	41.6	80.9	30.7	31.2	25.8
9	0.06	0.98	103.5	200.0	50.0	50.1	66.3	38.1	29.0	8.4
10	0.06	0.35	103.5	200.0	50.0	52.1	98.3	15.2	15.4	20.6
11	0.06	0.68	103.5	200.0	50.0	61.8	88.2	25.1	10.0	5.1
12	0.06	0.40	103.5	200.0	50.0	60.9	109.6	15.2	25.7	20.0
13	0.06	0.97	103.5	200.0	50.0	73.5	91.7	36.3	24.4	9.9
14	0.06	0.42	103.5	200.0	50.0	76.9	120.4	16.5	25.0	15.2
15	0.06	0.81	103.5	200.0	50.0	82.7	107.6	34.4	31.0	15.1
16	0.06	0.90	103.5	200.0	50.0	62.6	86.0	41.1	35.5	20.1
1	0.05	0.91	103.5	200.0	50.0	9.8	25.0	39.4	17.7	10.6
2	0.05	0.66	103.5	200.0	50.0	11.2	41.1	39.1	27.7	21.5
3	0.05	0.46	103.5	200.0	50.0	20.7	56.8	20.8	16.9	10.2
4	0.05	0.82	103.5	200.0	50.0	20.3	40.7	46.3	26.0	24.5
5	0.05	0.94	103.5	200.0	50.0	32.0	47.7	39.9	26.1	10.3
6	0.05	0.43	103.5	200.0	50.0	31.0	66.8	25.6	15.7	20.6
7	0.05	0.43	103.5	200.0	50.0	40.8	78.2	20.2	15.2	15.2
8	0.05	0.52	103.5	200.0	50.0	41.2	80.6	30.4	31.9	25.4
9	0.05	0.86	103.5	200.0	50.0	62.9	81.3	35.5	20.8	10.2
10	0.05	0.30	103.5	200.0	50.0	51.3	97.9	15.0	15.4	20.5
11	0.05	0.88	103.5	200.0	50.0	62.9	79.8	33.3	10.4	5.1
12	0.05	0.35	103.5	200.0	50.0	57.7	105.9	15.7	27.2	18.8
13	0.05	0.69	103.5	200.0	50.0	71.6	97.4	29.8	25.1	10.3
14	0.05	0.32	103.5	200.0	50.0	71.9	119.7	15.1	30.3	15.1
15	0.05	0.72	103.5	200.0	50.0	83.5	108.5	34.1	30.9	15.2
16	0.05	0.41	103.5	200.0	50.0	82.6	128.4	24.7	41.1	25.7

Table G.2: Results from the optimisation process for massless circular objects ranging from 60mm to 120mm diameter and a horizontal displacement of ±6mm. The starting value sets can be found in Table 4. The fixed design parameters used in the optimisation process were L_0, L_1 and L_2. A Q-value of 1.00 represents a complete feasible grasp range for the presented design parameters and coefficient of friction (μ).

Starting value set	μ	Q	L_0 [mm]	L_1 [mm]	L_2 [mm]	L_3 [mm]	L_5 [mm]	L_6 [mm]	L_7 [mm]	L_8 [mm]
1	0.05	0.98	103.5	218.0	50.0	10.4	25.4	39.7	19.4	9.4
2	0.05	0.67	103.5	218.0	50.0	8.5	40.7	47.3	25.5	36.7
3	0.05	0.58	103.5	218.0	50.0	19.0	52.4	21.8	12.8	11.2
4	0.05	1.00	103.5	218.0	50.0	18.5	40.9	45.7	33.2	20.5
5	0.05	0.98	103.5	218.0	50.0	31.2	48.0	39.2	25.7	10.2
6	0.05	1.00	103.5	218.0	50.0	10.6	28.3	43.6	29.2	13.9
7	0.05	0.45	103.5	218.0	50.0	40.6	77.8	20.5	15.2	15.1
8	0.05	0.57	103.5	218.0	50.0	42.3	80.1	31.4	31.4	25.3
9	0.05	0.55	103.5	218.0	50.0	51.6	85.4	25.5	30.6	10.3
10	0.05	0.31	103.5	218.0	50.0	52.0	98.5	14.7	15.3	20.3
11	0.05	0.70	103.5	218.0	50.0	62.0	87.8	25.4	10.1	5.1
12	0.05	0.36	103.5	218.0	50.0	61.7	110.3	14.8	26.2	19.5
13	0.05	0.76	103.5	218.0	50.0	72.3	97.9	29.9	25.5	10.2
14	0.05	0.40	103.5	218.0	50.0	72.0	118.9	15.3	30.3	15.1
15	0.05	0.76	103.5	218.0	50.0	83.4	108.4	34.0	31.0	15.1
16	0.05	0.62	103.5	218.0	50.0	79.4	109.4	39.0	37.9	27.3
1	0.04	0.89	103.5	218.0	50.0	11.7	27.1	38.8	18.6	9.5
2	0.04	0.83	103.5	218.0	50.0	11.7	31.3	46.3	25.2	22.7
3	0.04	0.46	103.5	218.0	50.0	21.4	57.9	19.7	15.9	10.2
4	0.04	0.59	103.5	218.0	50.0	20.2	49.8	39.1	25.8	25.7
5	0.04	0.91	103.5	218.0	50.0	31.3	47.8	39.4	26.0	10.4
6	0.04	0.37	103.5	218.0	50.0	30.8	67.1	24.6	15.9	20.3
7	0.04	0.36	103.5	218.0	50.0	41.2	78.8	19.9	15.3	15.3
8	0.04	0.89	103.5	218.0	50.0	47.4	63.3	39.0	39.6	3.5
9	0.04	0.84	103.5	218.0	50.0	48.0	66.2	35.2	22.9	8.2
10	0.04	0.26	103.5	218.0	50.0	51.5	97.1	15.0	15.2	19.7
11	0.04	0.62	103.5	218.0	50.0	61.6	87.8	24.9	10.2	5.1
12	0.04	0.31	103.5	218.0	50.0	61.2	109.2	14.9	26.5	19.6
13	0.04	0.68	103.5	218.0	50.0	72.0	97.6	29.8	25.6	10.2
14	0.04	0.33	103.5	218.0	50.0	72.4	118.7	15.1	30.2	15.1
15	0.04	0.66	103.5	218.0	50.0	82.7	107.9	33.7	31.5	15.1
16	0.04	0.37	103.5	218.0	50.0	82.1	127.3	25.1	41.5	25.4

Table G.3: Results from the optimisation process for massless circular objects ranging from 60mm to 120mm diameter and a horizontal displacement of ±6mm. The starting value sets can be found in Table 4. The fixed design parameters used in the optimisation process were L_0, L_1 and L_2. A Q-value of 1.00 represents a complete feasible grasp range for the presented design parameters and coefficient of friction (μ).

Starting value set	μ	Q	L_0 [mm]	L_1 [mm]	L_2 [mm]	L_3 [mm]	L_5 [mm]	L_6 [mm]	L_7 [mm]	L_8 [mm]
1	0.04	0.91	103.5	223.0	50.0	11.8	26.7	38.9	18.3	8.8
2	0.04	0.79	103.5	223.0	50.0	11.6	32.3	45.2	24.5	23.0
3	0.04	0.45	103.5	223.0	50.0	20.7	58.1	19.3	16.8	10.2
4	0.04	0.97	103.5	223.0	50.0	16.7	37.3	45.6	33.5	18.3
5	0.04	0.92	103.5	223.0	50.0	31.3	48.7	38.8	25.8	10.3
6	0.04	0.38	103.5	223.0	50.0	30.8	66.3	25.5	15.6	20.7
7	0.04	0.38	103.5	223.0	50.0	39.8	77.2	20.4	15.5	15.5
8	0.04	0.47	103.5	223.0	50.0	40.9	79.9	30.5	32.0	25.6
9	0.04	0.50	103.5	223.0	50.0	52.8	86.2	25.4	31.1	10.1

Continued on Next Page...

Table G.3 – Continued

Starting value set	μ	Q	L_0 [mm]	L_1 [mm]	L_2 [mm]	L_3 [mm]	L_5 [mm]	L_6 [mm]	L_7 [mm]	L_8 [mm]
10	0.04	0.26	103.5	223.0	50.0	51.8	97.8	15.5	15.3	20.2
11	0.04	0.63	103.5	223.0	50.0	62.2	88.3	24.9	10.3	5.1
12	0.04	0.31	103.5	223.0	50.0	61.2	109.5	15.0	25.4	20.3
13	0.04	0.68	103.5	223.0	50.0	72.3	97.8	29.8	25.5	10.2
14	0.04	0.35	103.5	223.0	50.0	71.9	118.1	15.2	30.3	15.2
15	0.04	0.71	103.5	223.0	50.0	81.9	103.2	37.0	30.5	15.3
16	0.04	0.38	103.5	223.0	50.0	81.0	126.7	25.0	42.0	26.0
1	0.04	0.93	103.5	227.0	50.0	10.8	24.8	40.0	20.2	8.4
2	0.04	1.00	103.5	227.0	50.0	5.2	25.8	50.1	31.9	22.7
3	0.04	0.53	103.5	227.0	50.0	23.6	55.1	23.8	15.0	11.5
4	0.04	1.00	103.5	227.0	50.0	14.9	40.9	49.4	45.5	21.2
5	0.04	0.93	103.5	227.0	50.0	31.5	49.0	38.8	26.4	10.4
6	0.04	0.92	103.5	227.0	50.0	42.7	57.7	36.2	20.7	4.9
7	0.04	0.38	103.5	227.0	50.0	40.6	78.0	20.2	15.3	15.2
8	0.04	0.47	103.5	227.0	50.0	41.3	80.6	29.8	31.6	25.6
9	0.04	0.50	103.5	227.0	50.0	51.9	86.1	24.9	31.3	10.2
10	0.04	0.26	103.5	227.0	50.0	51.7	98.0	15.1	15.6	20.5
11	0.04	0.85	103.5	227.0	50.0	65.5	83.7	32.2	9.4	4.9
12	0.04	0.31	103.5	227.0	50.0	60.3	108.4	15.0	26.4	19.6
13	0.04	0.70	103.5	227.0	50.0	71.9	97.2	30.0	25.6	10.2
14	0.04	0.36	103.5	227.0	50.0	70.4	115.4	16.2	30.2	15.1
15	0.04	0.93	103.5	227.0	50.0	94.1	111.4	37.0	35.3	7.0
16	0.04	0.39	103.5	227.0	50.0	82.5	127.2	25.1	41.1	25.2
1	0.04	0.92	103.5	228.0	50.0	12.1	26.8	39.3	18.7	8.9
2	0.04	0.99	103.5	228.0	50.0	10.5	31.6	48.3	31.9	21.9
3	0.04	0.47	103.5	228.0	50.0	22.0	60.2	18.5	16.3	10.4
4	0.04	0.92	103.5	228.0	50.0	21.5	42.3	47.3	33.8	21.8
5	0.04	0.93	103.5	228.0	50.0	31.7	48.4	39.5	26.4	10.3
6	0.04	0.40	103.5	228.0	50.0	31.0	63.4	28.2	15.0	20.9
7	0.04	0.38	103.5	228.0	50.0	40.9	78.1	20.3	15.4	15.2
8	0.04	0.91	103.5	228.0	50.0	42.6	63.6	39.9	49.0	5.2
9	0.04	0.51	103.5	228.0	50.0	51.8	85.5	25.3	31.1	10.2
10	0.04	0.26	103.5	228.0	50.0	50.6	98.2	15.1	15.2	20.5
11	0.04	0.88	103.5	228.0	50.0	70.6	88.4	32.3	9.0	4.2
12	0.04	0.32	103.5	228.0	50.0	61.1	109.3	14.9	26.4	19.8
13	0.04	0.70	103.5	228.0	50.0	72.0	97.4	29.8	25.6	10.1
14	0.04	0.36	103.5	228.0	50.0	71.0	116.1	15.9	30.1	15.1
15	0.04	0.93	103.5	228.0	50.0	92.5	110.7	36.8	34.6	8.1
16	0.04	0.94	103.5	228.0	50.0	76.0	104.1	42.2	60.9	16.2
1	0.03	0.76	103.5	227.0	50.0	10.1	25.8	39.2	18.9	10.4
2	0.03	0.07	103.5	227.0	50.0	10.2	51.0	42.8	25.5	20.4
3	0.03	0.08	103.5	227.0	50.0	20.0	70.0	20.0	15.8	10.0
4	0.03	0.88	103.5	227.0	50.0	17.1	39.1	48.4	39.5	20.7
5	0.03	0.79	103.5	227.0	50.0	31.3	49.2	38.3	26.1	10.4
6	0.03	0.40	103.5	227.0	50.0	26.7	63.2	25.3	24.7	17.0
7	0.03	0.28	103.5	227.0	50.0	41.3	79.5	19.4	15.5	15.4
8	0.03	0.47	103.5	227.0	50.0	41.9	78.6	30.5	37.2	19.5
9	0.03	0.45	103.5	227.0	50.0	53.6	87.2	24.9	30.3	10.3
10	0.03	0.20	103.5	227.0	50.0	51.8	98.6	14.8	14.5	20.7
11	0.03	0.54	103.5	227.0	50.0	62.6	88.8	24.6	10.3	5.0
12	0.03	0.23	103.5	227.0	50.0	60.4	108.8	15.2	25.5	20.2
13	0.03	0.59	103.5	227.0	50.0	72.0	97.4	29.8	25.6	10.0
14	0.03	0.28	103.5	227.0	50.0	71.4	117.2	15.3	30.3	15.1
15	0.03	0.60	103.5	227.0	50.0	82.7	105.2	35.7	31.1	14.5
16	0.03	0.30	103.5	227.0	50.0	82.8	128.0	24.7	41.1	25.4

APPENDIX H MINIMUM REQUIRED FRICTION FORCES - RESULTS OPTIMISATION PROCESS

Table H.1: Results from the optimisation process for circular objects ranging from 60mm to 120mm diameter and a horizontal displacement of ±6mm. The starting value sets can be found in Table 4. The fixed design parameters used in the optimisation process are $L_0 = 103.5$mm, $L_1 = 200$mm and $L_2 = 50$mm. A Q-value of 1.00 represents a complete feasible grasp range for the presented coefficient of friction (μ), actuation torque (T_a) and design parameters (L_3, L_5, L_6, L_7 and L_8).

Starting value set	μ	Q	T_a	Max F_{p1_t} [N]	Max F_{p2_t} [N]	Total F_{p_t} [N]	L_3 [mm]	L_5 [mm]	L_6 [mm]	L_7 [mm]	L_8 [mm]
1	0.30	0.99	600	−−	−−	−−	11.7	44.3	35.8	8.9	9.8
2	0.30	1.00	600	1.680	0.397	3.361	7.4	65.3	34.3	8.4	20.9
3	0.30	0.98	600	−−	−−	−−	22.3	58.0	27.2	8.0	10.9
4	0.30	1.00	600	1.512	0.220	3.025	24.5	47.3	47.5	13.1	29.2
5	0.30	0.98	600	−−	−−	−−	31.0	52.8	44.2	22.8	9.9
6	0.30	1.00	600	1.980	0.489	4.068	35.0	70.9	27.9	9.3	20.6
7	0.30	0.99	600	−−	−−	−−	44.3	89.0	18.7	7.5	20.7
8	0.30	0.99	600	−−	−−	−−	42.4	79.4	35.2	16.3	29.0
9	0.30	1.00	600	1.345	0.443	2.689	62.0	71.8	43.2	12.0	8.5
10	0.30	0.90	600	−−	−−	−−	52.2	99.3	15.6	13.9	21.3
11	0.30	0.89	600	−−	−−	−−	59.1	91.5	25.8	9.6	5.2
12	0.30	0.97	600	−−	−−	−−	58.3	108.5	18.9	13.1	26.1
13	0.30	0.96	600	−−	−−	−−	67.5	93.2	35.5	22.0	10.1
14	0.30	0.96	600	−−	−−	−−	70.3	114.5	20.4	11.1	20.7
15	0.30	0.96	600	−−	−−	−−	80.9	110.6	36.3	29.3	15.2
16	0.30	0.95	600	−−	−−	−−	92.1	132.9	29.9	26.3	27.0
1	0.30	1.00	800	2.182	0.646	4.522	10.6	38.9	36.3	16.2	10.0
2	0.30	1.00	800	1.672	0.417	3.343	10.8	50.1	49.7	20.3	20.8
3	0.30	1.00	800	2.734	0.668	5.544	22.1	53.7	25.3	9.6	11.3
4	0.30	1.00	800	1.861	0.422	3.726	20.8	51.0	43.5	22.3	24.8
5	0.30	1.00	800	1.909	0.464	3.818	30.0	50.0	40.0	25.0	10.0
6	0.30	1.00	800	2.948	1.094	6.663	30.0	70.0	25.0	15.0	20.0
7	0.30	1.00	800	3.010	1.068	6.490	42.9	85.1	22.7	11.1	15.8
8	0.30	1.00	800	2.294	0.567	4.589	46.1	87.6	33.6	23.6	25.8
9	0.30	1.00	800	2.104	0.535	4.209	58.8	83.5	35.5	25.5	9.4
10	0.30	1.00	800	3.728	1.482	8.475	53.6	100.3	18.1	9.7	20.8
11	0.30	1.00	800	2.369	0.667	4.825	58.1	85.2	29.1	9.5	5.0
12	0.30	1.00	800	3.472	1.522	8.294	66.4	109.6	20.2	11.5	19.9
13	0.30	1.00	800	2.385	0.830	5.129	69.1	102.2	31.7	24.0	10.1
14	0.30	1.00	800	3.341	1.312	7.756	72.6	112.8	20.9	9.3	17.8
15	0.30	1.00	800	2.130	0.536	4.261	80.0	110.0	35.0	30.0	15.0
16	0.30	1.00	800	2.810	1.060	6.455	90.2	132.9	27.6	26.6	25.8
1	0.30	1.00	1000	3.229	1.253	7.489	10.3	36.0	30.9	18.0	10.3
2	0.30	1.00	1000	2.370	0.762	5.049	10.0	50.0	45.0	25.0	20.0
3	0.30	1.00	1000	3.835	1.749	9.237	21.3	57.0	22.9	14.1	10.8
4	0.30	1.00	1000	2.619	0.624	5.453	20.0	50.0	40.0	25.0	25.0
5	0.30	1.00	1000	1.943	0.549	3.886	30.0	50.0	40.0	25.0	10.0
6	0.30	1.00	1000	3.431	0.854	6.862	30.0	70.0	25.0	15.0	20.0
7	0.30	1.00	1000	4.217	1.950	10.180	39.3	79.9	21.0	14.5	15.8
8	0.30	1.00	1000	3.181	1.297	7.247	42.4	88.8	31.8	28.7	23.2
9	0.30	1.00	1000	3.329	1.326	7.663	52.0	82.9	29.1	24.2	10.7
10	0.30	1.00	1000	5.377	2.610	13.263	51.6	99.5	16.0	12.4	21.8
11	0.30	1.00	1000	3.426	1.395	7.860	60.0	90.0	25.0	10.0	5.0
12	0.30	1.00	1000	4.594	1.368	9.629	64.4	114.2	19.4	16.0	26.2
13	0.30	1.00	1000	3.158	0.788	6.316	70.0	100.0	30.0	25.0	10.0
14	0.30	1.00	1000	4.118	1.595	9.206	70.4	111.8	21.1	12.1	15.4
15	0.30	1.00	1000	2.220	0.639	4.440	80.0	110.0	35.0	30.0	15.0
16	0.30	1.00	1000	3.504	1.427	8.034	84.0	132.1	28.1	33.9	25.5

Continued on Next Page...

Table H.1 – Continued

Starting value set	μ	Q	T_a	Max F_{p1_t} [N]	Max F_{p2_t} [N]	Total F_{p_t} [N]	L_3 [mm]	L_5 [mm]	L_6 [mm]	L_7 [mm]	L_8 [mm]
1	0.30	1.00	1200	4.070	1.645	9.654	10.0	35.0	30.0	20.0	10.0
2	0.30	1.00	1200	2.562	0.704	5.125	10.0	50.0	45.0	25.0	20.0
3	0.30	1.00	1200	4.810	2.204	11.379	21.0	61.2	22.0	14.9	10.3
4	0.30	1.00	1200	2.838	0.599	5.682	20.0	50.0	40.0	25.0	25.0
5	0.30	1.00	1200	1.977	0.636	3.954	30.0	50.0	40.0	25.0	10.0
6	0.30	1.00	1200	3.761	1.006	7.525	30.0	70.0	25.0	15.0	20.0
7	0.30	1.00	1200	5.318	2.475	12.934	40.0	80.0	20.0	15.0	15.0
8	0.30	1.00	1200	4.120	1.906	9.810	40.0	90.0	30.0	30.0	25.0
9	0.30	1.00	1200	4.200	1.823	9.999	50.1	81.5	28.3	27.6	10.6
10	0.30	0.99	1200	−−	−−	−−	50.3	98.5	15.6	14.2	21.0
11	0.30	1.00	1200	3.995	1.043	7.991	60.0	90.0	25.0	10.0	5.0
12	0.30	1.00	1200	6.107	2.739	14.141	59.4	110.3	17.6	15.8	23.1
13	0.30	1.00	1200	3.433	0.925	6.873	70.0	100.0	30.0	25.0	10.0
14	0.30	1.00	1200	5.636	2.856	14.236	61.5	104.6	19.5	17.6	19.3
15	0.30	1.00	1200	2.390	0.745	4.786	80.0	110.0	35.0	30.0	15.0
16	0.30	1.00	1200	4.383	1.783	10.099	81.4	129.6	27.2	35.6	25.5
1	0.30	1.00	1400	4.697	1.275	9.919	10.0	35.0	30.0	20.0	10.0
2	0.30	1.00	1400	2.693	0.803	5.389	10.0	50.0	45.0	25.0	20.0
3	0.30	1.00	1400	5.932	2.721	13.815	20.3	64.5	21.3	14.9	10.6
4	0.30	1.00	1400	3.017	0.674	6.034	20.0	50.0	40.0	25.0	25.0
5	0.30	1.00	1400	2.011	0.722	4.021	30.0	50.0	40.0	25.0	10.0
6	0.30	1.00	1400	4.093	1.152	8.186	30.0	70.0	25.0	15.0	20.0
7	0.30	1.00	1400	6.153	2.244	13.745	40.0	80.0	20.0	15.0	15.0
8	0.30	1.00	1400	4.756	1.580	10.101	40.0	90.0	30.0	30.0	25.0
9	0.30	1.00	1400	4.940	1.558	10.608	53.8	85.0	27.4	26.1	10.1
10	0.30	1.00	1400	7.581	3.531	17.981	50.9	99.5	16.1	14.1	20.7
11	0.30	1.00	1400	4.368	1.192	8.735	60.0	90.0	25.0	10.0	5.0
12	0.30	1.00	1400	6.486	1.834	12.973	57.8	106.6	18.9	15.4	21.6
13	0.30	1.00	1400	3.712	1.053	7.424	70.0	100.0	30.0	25.0	10.0
14	0.30	1.00	1400	6.525	2.889	15.361	70.8	114.4	19.2	16.3	17.4
15	0.30	1.00	1400	2.863	0.851	5.734	80.0	110.0	35.0	30.0	15.0
16	0.30	1.00	1400	5.451	2.425	12.790	82.4	133.9	25.8	36.0	25.8
1	0.30	1.00	1600	5.234	1.137	10.467	10.0	35.0	30.0	20.0	10.0
2	0.30	1.00	1600	2.827	0.895	5.654	10.0	50.0	45.0	25.0	20.0
3	0.30	1.00	1600	6.909	3.147	16.174	20.6	63.0	20.6	15.4	10.3
4	0.30	1.00	1600	3.196	0.749	6.393	20.0	50.0	40.0	25.0	25.0
5	0.30	1.00	1600	2.052	0.808	4.118	30.0	50.0	40.0	25.0	10.0
6	0.30	1.00	1600	4.425	1.296	8.851	30.0	70.0	25.0	15.0	20.0
7	0.30	1.00	1600	6.988	2.013	14.556	40.0	80.0	20.0	15.0	15.0
8	0.30	1.00	1600	5.316	1.445	10.633	40.0	90.0	30.0	30.0	25.0
9	0.30	1.00	1600	6.038	2.564	14.080	52.1	87.3	26.1	27.4	10.4
10	0.30	1.00	1600	9.075	4.411	22.166	51.3	99.0	15.4	14.3	20.5
11	0.30	1.00	1600	4.736	1.351	9.472	60.0	90.0	25.0	10.0	5.0
12	0.30	1.00	1600	8.171	3.185	18.022	58.7	109.6	17.8	17.7	23.5
13	0.30	1.00	1600	3.987	1.193	7.980	70.0	100.0	30.0	25.0	10.0
14	0.30	1.00	1600	7.380	2.704	16.318	71.2	114.2	19.3	16.2	17.2
15	0.30	1.00	1600	3.336	0.947	6.681	80.0	110.0	35.0	30.0	15.0
16	0.30	1.00	1600	6.230	3.092	15.406	80.0	130.0	26.3	40.0	25.0
1	0.20	0.89	600	−−	−−	−−	13.4	39.7	30.9	4.6	12.1
2	0.20	0.67	600	−−	−−	−−	10.6	45.8	48.9	23.5	19.8
3	0.20	0.83	600	−−	−−	−−	26.2	57.4	26.2	6.1	13.1
4	0.20	0.82	600	−−	−−	−−	24.3	52.4	42.1	15.4	26.6
5	0.20	0.85	600	−−	−−	−−	34.4	38.0	50.6	20.8	9.5
6	0.20	0.78	600	−−	−−	−−	30.6	70.9	26.0	13.6	20.8
7	0.20	0.78	600	−−	−−	−−	39.3	80.0	21.3	10.0	19.1

Continued on Next Page...

Table H.1 – Continued

Starting value set	μ	Q	T_a	Max F_{p1_t} [N]	Max F_{p2_t} [N]	Total F_{p_t} [N]	L_3 [mm]	L_5 [mm]	L_6 [mm]	L_7 [mm]	L_8 [mm]
8	0.20	0.78	600	−−	−−	−−	46.9	84.2	33.9	21.5	27.6
9	0.20	0.88	600	−−	−−	−−	43.9	56.3	43.9	10.6	12.9
10	0.20	0.74	600	−−	−−	−−	53.3	100.6	16.9	12.2	20.3
11	0.20	0.69	600	−−	−−	−−	60.0	90.3	25.9	9.9	5.1
12	0.20	0.73	600	−−	−−	−−	61.9	110.8	17.9	17.0	23.6
13	0.20	0.72	600	−−	−−	−−	70.0	100.0	31.5	25.0	10.0
14	0.20	0.72	600	−−	−−	−−	73.7	119.0	18.4	15.2	19.4
15	0.20	0.76	600	−−	−−	−−	80.2	109.9	35.0	30.1	15.4
16	0.20	0.73	600	−−	−−	−−	83.5	131.3	27.9	33.6	29.7
1	0.20	0.99	800	−−	−−	−−	14.5	37.0	34.3	6.1	12.2
2	0.20	0.99	800	−−	−−	−−	14.3	20.1	54.2	22.1	16.6
3	0.20	0.98	800	−−	−−	−−	22.3	41.9	34.7	4.5	9.4
4	0.20	0.94	800	−−	−−	−−	24.3	49.5	43.5	16.6	25.5
5	0.20	1.00	800	1.080	0.728	2.161	32.6	37.7	49.5	23.7	9.9
6	0.20	0.87	800	−−	−−	−−	32.3	72.7	25.3	13.4	20.3
7	0.20	0.90	800	−−	−−	−−	42.9	71.1	30.2	9.6	15.1
8	0.20	1.00	800	1.423	0.325	2.846	50.4	61.0	47.7	17.6	14.7
9	0.20	1.00	800	1.173	0.803	2.347	70.2	77.0	44.3	11.5	6.2
10	0.20	0.79	800	−−	−−	−−	51.5	98.2	17.0	12.9	20.5
11	0.20	0.78	800	−−	−−	−−	60.1	89.9	25.7	10.1	5.0
12	0.20	0.78	800	−−	−−	−−	61.9	111.5	17.9	17.4	22.8
13	0.20	1.00	800	1.167	0.211	2.333	76.2	87.4	45.3	21.5	11.6
14	0.20	0.78	800	−−	−−	−−	74.9	117.3	19.8	15.3	19.1
15	0.20	0.87	800	−−	−−	−−	81.4	110.0	35.1	30.4	15.3
16	0.20	0.80	800	−−	−−	−−	86.9	130.1	27.2	30.7	26.5
1	0.20	1.00	1000	1.897	0.588	3.794	7.5	37.6	27.8	7.1	12.9
2	0.20	1.00	1000	1.424	0.451	2.849	15.6	30.5	47.7	18.0	19.3
3	0.20	0.99	1000	−−	−−	−−	22.5	52.3	27.5	6.4	11.9
4	0.20	1.00	1000	1.415	0.302	3.022	23.4	44.3	47.1	21.8	20.5
5	0.20	1.00	1000	1.508	0.347	3.016	30.5	47.8	43.2	24.8	10.0
6	0.20	0.95	1000	−−	−−	−−	31.5	69.7	26.5	12.7	21.2
7	0.20	0.98	1000	−−	−−	−−	34.9	64.4	29.9	10.5	15.7
8	0.20	0.93	1000	−−	−−	−−	47.5	84.0	33.3	21.7	26.4
9	0.20	1.00	1000	1.453	0.356	2.906	36.3	52.5	42.8	20.1	13.2
10	0.20	0.83	1000	−−	−−	−−	51.6	100.0	16.4	13.3	20.8
11	0.20	1.00	1000	2.502	2.140	6.358	67.1	83.5	35.6	6.4	7.5
12	0.20	0.81	1000	−−	−−	−−	59.0	108.6	17.6	17.8	24.1
13	0.20	1.00	1000	1.511	0.390	3.021	75.4	91.3	39.5	19.4	9.2
14	0.20	0.82	1000	−−	−−	−−	85.0	124.0	20.4	11.9	15.8
15	0.20	0.94	1000	−−	−−	−−	81.5	109.3	35.4	30.2	15.2
16	0.20	0.85	1000	−−	−−	−−	84.8	129.3	27.0	31.7	26.6
1	0.20	1.00	1200	1.995	0.606	3.990	8.6	34.9	36.8	12.7	13.2
2	0.20	1.00	1200	1.817	0.471	3.667	13.7	38.3	44.3	16.6	23.2
3	0.20	1.00	1200	2.607	0.755	5.214	20.9	50.5	26.9	7.6	12.4
4	0.20	1.00	1200	1.812	0.499	3.623	21.9	48.5	44.4	23.1	22.7
5	0.20	1.00	1200	1.998	0.582	3.996	30.0	50.0	40.0	25.0	10.0
6	0.20	0.99	1200	−−	−−	−−	28.6	63.4	30.9	14.7	22.4
7	0.20	0.99	1200	−−	−−	−−	36.6	69.9	28.4	13.0	17.8
8	0.20	0.97	1200	−−	−−	−−	45.5	82.6	33.1	22.4	26.8
9	0.20	1.00	1200	1.898	0.594	3.796	64.0	83.0	36.1	17.9	6.2
10	0.20	0.84	1200	−−	−−	−−	50.1	98.8	16.3	13.9	21.5
11	0.20	0.88	1200	−−	−−	−−	60.5	89.7	25.6	10.1	5.1
12	0.20	0.82	1200	−−	−−	−−	64.9	114.8	17.6	20.0	24.4
13	0.20	1.00	1200	2.252	0.710	4.504	72.4	96.1	33.8	18.9	10.4
14	0.20	1.00	1200	4.656	3.811	11.715	58.8	71.1	39.3	17.7	7.2

Continued on Next Page...

Table H.1 – Continued

Starting value set	μ	Q	T_a	Max F_{p1_t} [N]	Max F_{p2_t} [N]	Total F_{p_t} [N]	L_3 [mm]	L_5 [mm]	L_6 [mm]	L_7 [mm]	L_8 [mm]
15	0.20	0.99	1200	−−	−−	−−	81.5	109.2	35.3	30.3	15.1
16	0.20	1.00	1200	2.683	0.800	5.365	88.1	114.9	40.1	34.7	22.4
1	0.20	1.00	1400	2.395	0.793	4.789	9.1	36.2	38.0	16.3	9.7
2	0.20	1.00	1400	2.034	0.609	4.071	12.0	38.6	44.3	19.6	23.6
3	0.20	1.00	1400	3.136	1.047	6.406	21.2	52.8	25.6	8.8	11.8
4	0.20	1.00	1400	2.191	0.678	4.384	20.3	51.4	42.7	23.8	23.9
5	0.20	1.00	1400	2.027	0.680	4.054	30.0	50.0	40.0	25.0	10.0
6	0.20	0.99	1400	−−	−−	−−	30.3	69.4	27.0	14.1	21.6
7	0.20	1.00	1400	3.370	1.180	7.033	28.6	64.9	25.4	11.1	18.3
8	0.20	0.99	1400	−−	−−	−−	44.8	84.3	32.4	23.4	27.5
9	0.20	1.00	1400	2.031	0.699	4.062	62.3	77.2	38.3	23.9	7.0
10	0.20	0.88	1400	−−	−−	−−	50.9	97.0	18.2	13.9	21.3
11	0.20	1.00	1400	2.579	0.827	5.158	67.2	86.2	31.9	6.3	4.1
12	0.20	1.00	1400	2.965	0.859	5.945	53.2	81.0	29.9	12.7	13.6
13	0.20	1.00	1400	2.699	0.856	5.405	74.7	98.6	33.1	21.3	10.1
14	0.20	0.88	1400	−−	−−	−−	74.1	113.1	20.9	13.7	16.9
15	0.20	1.00	1400	2.664	0.817	5.400	84.0	110.0	35.0	30.0	15.0
16	0.20	1.00	1400	2.871	0.847	5.749	83.2	115.5	36.6	35.2	23.8
1	0.20	1.00	1600	3.117	1.131	6.317	10.5	39.9	32.4	14.7	9.8
2	0.20	1.00	1600	2.265	0.718	4.534	11.8	40.6	45.3	24.7	20.2
3	0.20	1.00	1600	3.423	1.182	6.847	21.7	55.1	25.7	9.9	11.8
4	0.20	1.00	1600	2.656	0.848	5.456	20.6	51.4	41.1	24.5	23.9
5	0.20	1.00	1600	2.054	0.783	4.118	30.0	50.0	40.0	25.0	10.0
6	0.20	1.00	1600	3.892	1.369	8.122	31.2	69.0	26.0	13.6	20.8
7	0.20	0.99	1600	−−	−−	−−	37.7	73.7	24.8	11.9	16.9
8	0.20	0.99	1600	−−	−−	−−	47.0	85.6	32.8	24.7	27.8
9	0.20	1.00	1600	2.934	0.932	5.869	59.8	80.9	34.6	25.3	8.0
10	0.20	0.88	1600	−−	−−	−−	50.4	97.7	17.1	13.9	20.4
11	0.20	0.93	1600	−−	−−	−−	60.4	89.6	25.4	10.1	5.1
12	0.20	0.85	1600	−−	−−	−−	58.0	108.5	17.0	18.1	24.2
13	0.20	0.98	1600	−−	−−	−−	70.4	99.9	30.4	24.8	10.0
14	0.20	0.85	1600	−−	−−	−−	75.1	120.0	17.7	16.1	18.6
15	0.20	1.00	1600	2.809	0.872	5.619	84.0	110.0	35.0	30.0	15.0
16	0.20	1.00	1600	3.344	1.046	6.713	74.9	109.8	35.0	33.8	24.0
1	0.10	0.66	800	−−	−−	−−	11.9	30.6	37.6	11.6	11.8
2	0.10	0.45	800	−−	−−	−−	10.4	49.5	38.8	26.9	21.4
3	0.10	0.62	800	−−	−−	−−	18.3	44.0	31.0	10.8	12.7
4	0.10	0.60	800	−−	−−	−−	20.6	47.7	43.9	23.4	25.6
5	0.10	0.78	800	−−	−−	−−	36.8	41.4	51.2	21.9	11.5
6	0.10	0.54	800	−−	−−	−−	30.9	68.9	24.8	15.4	20.3
7	0.10	0.53	800	−−	−−	−−	40.1	79.8	20.5	14.8	15.3
8	0.10	0.60	800	−−	−−	−−	44.7	71.3	44.0	31.1	26.5
9	0.10	0.46	800	−−	−−	−−	52.6	88.8	26.4	28.9	10.1
10	0.10	0.45	800	−−	−−	−−	51.7	98.7	15.0	15.3	19.8
11	0.10	0.51	800	−−	−−	−−	61.3	88.8	25.4	10.2	5.1
12	0.10	0.47	800	−−	−−	−−	58.9	109.3	16.0	23.3	21.8
13	0.10	0.55	800	−−	−−	−−	71.6	99.3	30.2	25.5	10.1
14	0.10	0.54	800	−−	−−	−−	36.1	78.9	27.5	24.0	25.2
15	0.10	0.62	800	−−	−−	−−	82.3	108.5	34.8	30.4	15.1
16	0.10	0.50	800	−−	−−	−−	81.9	130.2	25.1	39.9	25.5
1	0.10	0.86	1000	−−	−−	−−	15.9	21.0	47.2	14.2	7.8
2	0.10	0.91	1000	−−	−−	−−	13.6	20.9	55.7	28.3	18.2
3	0.10	0.49	1000	−−	−−	−−	20.7	61.0	20.7	15.5	10.2
4	0.10	0.65	1000	−−	−−	−−	20.6	49.9	41.6	23.5	25.9
5	0.10	0.85	1000	−−	−−	−−	35.0	41.3	49.6	24.7	9.8

Continued on Next Page...

Table H.1 – Continued

Starting value set	μ	Q	T_a	Max F_{p1_t} [N]	Max F_{p2_t} [N]	Total F_{p_t} [N]	L_3 [mm]	L_5 [mm]	L_6 [mm]	L_7 [mm]	L_8 [mm]
6	0.10	0.57	1000	−−	−−	−−	31.0	68.5	24.9	15.4	20.1
7	0.10	0.56	1000	−−	−−	−−	40.3	79.8	20.3	15.2	15.2
8	0.10	0.55	1000	−−	−−	−−	41.3	86.4	28.9	31.0	25.8
9	0.10	0.63	1000	−−	−−	−−	51.4	79.5	28.9	16.4	12.6
10	0.10	0.48	1000	−−	−−	−−	51.5	98.7	15.1	15.3	19.9
11	0.10	0.87	1000	−−	−−	−−	67.1	73.2	43.8	8.3	4.4
12	0.10	0.47	1000	−−	−−	−−	59.2	110.8	15.5	24.3	20.5
13	0.10	0.61	1000	−−	−−	−−	71.7	99.3	30.1	25.4	10.1
14	0.10	0.42	1000	−−	−−	−−	71.3	121.4	16.0	28.2	15.6
15	0.10	0.68	1000	−−	−−	−−	83.3	108.7	35.1	30.2	15.2
16	0.10	0.53	1000	−−	−−	−−	81.1	129.3	25.0	40.2	25.7
1	0.10	0.87	1200	−−	−−	−−	10.7	20.2	45.0	12.1	11.2
2	0.10	0.55	1200	−−	−−	−−	10.4	47.3	38.6	27.4	20.6
3	0.10	0.78	1200	−−	−−	−−	19.7	39.4	33.1	7.8	8.2
4	0.10	0.70	1200	−−	−−	−−	20.6	49.9	41.2	24.1	25.2
5	0.10	0.95	1200	−−	−−	−−	33.9	40.5	48.5	26.0	9.9
6	0.10	0.59	1200	−−	−−	−−	30.8	68.5	25.0	15.3	20.3
7	0.10	0.58	1200	−−	−−	−−	40.4	79.8	20.3	15.2	15.2
8	0.10	0.59	1200	−−	−−	−−	40.9	84.7	29.9	30.8	26.3
9	0.10	0.51	1200	−−	−−	−−	52.4	90.0	25.1	29.7	10.1
10	0.10	0.49	1200	−−	−−	−−	51.5	97.6	16.1	15.1	20.1
11	0.10	0.61	1200	−−	−−	−−	62.3	89.0	25.8	9.9	5.0
12	0.10	0.51	1200	−−	−−	−−	60.4	110.6	16.2	24.0	21.5
13	0.10	0.66	1200	−−	−−	−−	72.3	99.6	30.2	24.9	10.1
14	0.10	0.42	1200	−−	−−	−−	68.6	117.7	16.3	29.5	15.6
15	0.10	0.72	1200	−−	−−	−−	83.0	108.8	34.9	30.4	15.2
16	0.10	0.55	1200	−−	−−	−−	81.5	129.3	25.1	40.3	25.4
1	0.10	0.67	1400	−−	−−	−−	10.6	36.8	32.8	17.5	10.1
2	0.10	0.73	1400	−−	−−	−−	11.5	40.0	38.7	17.8	24.0
3	0.10	0.55	1400	−−	−−	−−	20.6	59.9	20.3	15.2	10.5
4	0.10	0.73	1400	−−	−−	−−	20.8	49.8	41.1	24.1	25.1
5	0.10	0.98	1400	−−	−−	−−	31.1	40.9	46.6	22.7	11.9
6	0.10	0.61	1400	−−	−−	−−	30.8	68.8	24.5	15.4	20.5
7	0.10	0.60	1400	−−	−−	−−	40.4	79.6	20.3	15.5	15.0
8	0.10	0.61	1400	−−	−−	−−	41.2	84.0	30.1	30.7	26.3
9	0.10	0.96	1400	−−	−−	−−	110.9	114.3	43.0	16.5	−0.3
10	0.10	0.49	1400	−−	−−	−−	50.0	97.3	15.2	15.5	20.6
11	0.10	0.62	1400	−−	−−	−−	61.5	89.0	25.0	10.1	5.1
12	0.10	0.50	1400	−−	−−	−−	60.3	110.7	15.8	24.4	20.0
13	0.10	0.69	1400	−−	−−	−−	72.0	98.9	30.5	25.4	10.2
14	0.10	1.00	1400	1.117	0.262	2.357	4.1	14.4	51.8	20.9	17.3
15	0.10	0.76	1400	−−	−−	−−	82.6	108.4	34.8	30.5	15.3
16	0.10	0.57	1400	−−	−−	−−	82.5	128.8	25.4	40.2	24.8
1	0.10	0.98	1600	−−	−−	−−	10.0	20.1	42.8	12.4	8.5
2	0.10	1.00	1600	1.305	0.403	3.238	12.1	24.8	52.0	24.5	18.9
3	0.10	0.76	1600	−−	−−	−−	10.6	41.5	27.5	10.8	14.9
4	0.10	0.99	1600	−−	−−	−−	23.5	37.1	50.0	25.7	19.0
5	0.10	0.99	1600	−−	−−	−−	33.2	43.0	45.6	26.7	10.0
6	0.10	0.63	1600	−−	−−	−−	30.7	67.7	25.1	15.3	20.4
7	0.10	0.61	1600	−−	−−	−−	40.4	79.6	20.1	15.4	14.9
8	0.10	0.79	1600	−−	−−	−−	32.1	51.4	48.6	22.7	26.7
9	0.10	0.99	1600	−−	−−	−−	65.8	77.2	41.0	16.8	7.8
10	0.10	0.51	1600	−−	−−	−−	50.7	97.2	15.5	15.3	19.8
11	0.10	0.66	1600	−−	−−	−−	61.9	88.9	25.4	9.9	5.1
12	0.10	0.53	1600	−−	−−	−−	59.6	109.8	16.0	23.7	21.0

Continued on Next Page...

Table H.1 – Continued

Starting value set	μ	Q	T_a	Max F_{p1_t} [N]	Max F_{p2_t} [N]	Total F_{p_t} [N]	L_3 [mm]	L_5 [mm]	L_6 [mm]	L_7 [mm]	L_8 [mm]
13	0.10	0.71	1600	−−	−−	−−	72.9	99.9	30.1	25.2	9.9
14	0.10	0.56	1600	−−	−−	−−	85.5	124.8	19.2	19.9	14.8
15	0.10	0.80	1600	−−	−−	−−	83.2	108.3	35.1	30.4	15.2
16	0.10	0.99	1600	−−	−−	−−	101.1	112.7	43.1	32.9	9.1
1	0.09	0.82	1400	−−	−−	−−	9.3	23.7	41.2	12.9	11.9
2	0.09	1.00	1400	0.908	0.506	1.817	13.3	23.0	55.7	28.2	20.3
3	0.09	0.92	1400	−−	−−	−−	17.0	21.4	43.6	13.8	2.1
4	0.09	0.95	1400	−−	−−	−−	21.4	32.5	56.5	27.9	23.6
5	0.09	0.95	1400	−−	−−	−−	32.5	40.0	47.1	24.5	9.9
6	0.09	0.57	1400	−−	−−	−−	30.7	66.6	26.1	15.3	20.2
7	0.09	0.56	1400	−−	−−	−−	39.8	78.9	20.2	15.8	14.7
8	0.09	0.58	1400	−−	−−	−−	41.8	85.0	29.9	31.3	26.1
9	0.09	0.98	1400	−−	−−	−−	19.2	28.6	49.8	31.1	13.2
10	0.09	0.45	1400	−−	−−	−−	51.4	98.7	14.9	15.3	20.4
11	0.09	0.60	1400	−−	−−	−−	62.0	89.0	25.3	10.1	5.1
12	0.09	0.49	1400	−−	−−	−−	60.1	109.2	16.3	24.0	20.2
13	0.09	0.84	1400	−−	−−	−−	91.6	104.7	38.8	20.8	7.2
14	0.09	0.50	1400	−−	−−	−−	79.5	121.3	19.0	23.4	16.3
15	0.09	0.73	1400	−−	−−	−−	82.9	107.8	35.3	30.3	15.2
16	0.09	0.54	1400	−−	−−	−−	82.3	128.4	25.7	40.2	25.2
1	0.09	0.96	1600	−−	−−	−−	10.7	18.3	44.9	19.0	7.2
2	0.09	0.92	1600	−−	−−	−−	14.0	25.4	54.9	22.5	24.0
3	0.09	0.67	1600	−−	−−	−−	22.0	52.7	25.7	11.9	12.0
4	0.09	0.71	1600	−−	−−	−−	20.6	49.3	41.2	24.5	25.3
5	0.09	0.98	1600	−−	−−	−−	33.1	42.0	46.0	27.0	9.8
6	0.09	0.57	1600	−−	−−	−−	31.0	68.3	24.8	15.4	20.6
7	0.09	0.57	1600	−−	−−	−−	40.3	79.2	20.2	15.7	14.7
8	0.09	0.61	1600	−−	−−	−−	42.3	83.4	30.8	31.0	25.3
9	0.09	0.96	1600	−−	−−	−−	72.7	82.0	42.1	18.7	6.3
10	0.09	0.46	1600	−−	−−	−−	52.6	98.2	15.8	14.9	19.7
11	0.09	0.62	1600	−−	−−	−−	62.0	88.9	25.4	10.2	5.1
12	0.09	0.49	1600	−−	−−	−−	59.9	110.1	15.7	24.3	20.4
13	0.09	0.69	1600	−−	−−	−−	73.8	100.0	30.6	24.7	9.9
14	0.09	0.50	1600	−−	−−	−−	79.0	122.5	17.9	24.4	16.6
15	0.09	0.76	1600	−−	−−	−−	82.8	106.9	35.6	30.3	15.2
16	0.09	0.55	1600	−−	−−	−−	82.4	128.8	25.4	40.6	24.8
1	0.08	0.78	1400	−−	−−	−−	10.5	24.6	41.1	13.5	11.3
2	0.08	0.98	1400	−−	−−	−−	15.6	26.6	58.9	28.9	25.4
3	0.08	0.48	1400	−−	−−	−−	21.3	58.0	21.7	16.1	10.2
4	0.08	0.63	1400	−−	−−	−−	20.5	49.4	40.6	24.5	25.3
5	0.08	0.75	1400	−−	−−	−−	31.6	48.8	40.2	25.8	9.9
6	0.08	0.50	1400	−−	−−	−−	30.7	68.3	24.8	15.4	20.5
7	0.08	0.50	1400	−−	−−	−−	40.8	79.6	20.0	15.4	14.9
8	0.08	0.54	1400	−−	−−	−−	41.8	83.2	30.3	31.1	25.7
9	0.08	0.92	1400	−−	−−	−−	44.7	51.2	46.7	33.2	6.2
10	0.08	0.40	1400	−−	−−	−−	51.5	98.3	15.1	15.2	19.8
11	0.08	0.56	1400	−−	−−	−−	62.0	88.9	25.2	10.0	5.0
12	0.08	0.44	1400	−−	−−	−−	60.0	110.0	15.8	25.0	20.0
13	0.08	0.79	1400	−−	−−	−−	97.5	113.3	37.2	19.9	8.5
14	0.08	0.42	1400	−−	−−	−−	73.2	122.4	14.7	25.2	18.5
15	0.08	0.69	1400	−−	−−	−−	82.7	106.7	35.7	30.4	15.2
16	0.08	0.49	1400	−−	−−	−−	81.8	127.8	25.4	40.9	24.8